



uc3m | Universidad **Carlos III** de Madrid

University Degree in Aerospace Engineering
Academic Year 2018-2019

Analysis of a high-lift device by boundary layer blowing system.

Bachelor Thesis

By

Martín López Meijide

Tutored and Supervised by

Pablo Fajardo Peña

July 2019



This work is licensed under Creative Commons
Attribution – Non Commercial – Non Derivatives

Abstract

Boundary layer control is a very important subject of investigation in fluid mechanics. The invention of high-lift devices in aircrafts has allowed to increase the capabilities of aerodynamic profiles. This thesis explores one opportunity of taking advantage of boundary layer control in turbulent regimes by means of a blowing system. Carefully CFD simulations have been performed with ANSYS Fluent at different angles of attack for the 2D NACA 4412 airfoil. The boundary conditions are sea level conditions for incompressible flow at Reynold number of 4.8 million, chord of 1m and Mach number of 0.2 for flow velocity. Three modifications of the airfoil geometry have been created at 61%, 50% and 39% of the chord. Each modification includes a slot for the blowing jet of height of 1% of the total chord. The results showed that the blowing system increases the lift coefficient and the aerodynamic efficiency at high angles of attack, which is very useful in take-off and landing configurations. The location of the blowing system at 50% of the chord showed to be the best location for the device. In conclusion, this high-lift device should be implemented and studied further in 3D cases, since it might be an innovative element not only in the aerospace industry, but also other fields of study like wind turbines or nautical ships.

Keywords: blowing system, boundary layer, CFD, airfoil, high-lift device.

Acknowledgments

I would like to express my gratitude to those people that have helped me during the development of this Bachelor Thesis. In particular:

To Ramón Robles Giménez, professor and inventor, for your constant help and support. With each debate that we have had, you made me conceive new situations and ideas, starting for the topic of this investigation. You have always been a fundamental support for me, my friend.

To Álvaro Jara-Rodelgo, Head of Airbus Proto Space. Since the first time that we talked on the phone you transmitted such an amazing enthusiasm for my idea and put all your interest in the development of my Thesis. Thanks for having the huge opportunity of learning from you.

To Pablo Fajardo Peña, PhD in Aeronautics and Tutor of this Bachelor Thesis. Thanks for being there since the very beginning and conception of the scope of this project. For your patience, your help and supervision on this Thesis. For every time that you listened to my concerns, doubts and ideas. It has been an honor being your pupil.

To professors Marco Raiola, Javier Rodríguez and Antonio Acosta, among others, that deserve my sincere gratitude. For all your suggestions and thoughts about the different possibilities of the research on the boundary layer and the CFD simulation.

I want to express my gratitude to all my family for the love and support received during all these years. Thanks to my parents for all the wisdom in living that I have received, and I always will. To my beloved sisters Ana and Marta, who give me joy and love every day of my life.

Moreover, above all, there is one person that has given all for me and, for who I want to dedicate this Thesis: my Mum. There are not enough words to express how much I love you.

Martín López Meijide,

July 2019.

Contents

1.	Introduction	13
1.1	State of the Art and Motivation	13
1.2	Objectives and hypothesis	19
2.	Theoretical background and Methodology	23
2.1	Turbulent Boundary Layer	23
2.2	Selection of the NACA profile	25
2.3	Computational Fluid Dynamics – ANSYS Fluent	28
3.	Results and Discussion	33
3.1	Data	33
3.2	Figures	41
4.	Conclusions	51
5.	Socio-economic context and Regulatory framework	55
	References	59

List of Figures:

1.1.	Description of Granados-Robles propeller [4, Figure 1].	15
1.2.	Cross-section description of Zarate's propeller [5, Figure 3].	15
1.3.	Boundary layer of the aerodynamic profile simulated with CFD without the invention (left) and with the invention (right). [5, Figures 6 and 7].	16
1.4.	Cross-section of the airfoil with Williams' embodiment [8, Figure 1].	17
1.5.	Sforza's blowing system for wind turbines [10, Figure 3].	17
1.6.	Blown boundary layer for supersonic engines [11, Figures 5 and 6].	18
1.7.	Side elevation view, showing a high adverse pressure gradient with detachment of the flow (left) and with the use of microjets (right), delaying separation [12, Figures 3 and 6].	18
1.9.	Effect of slot on airflow over an aerofoil [15, Figure 3.34]	20
1.10.	Velocity profile of the boundary layer	20
2.1.	Lift, Drag and Angle of Attack on the Airfoil [41, Figure 1].	26
2.2.	Geometry of the modified NACA 4412 with the blowing system.	27
2.3.	Lift coefficient vs number of mesh nodes.	30
2.4.	Drag coefficient vs number of mesh nodes.	30
2.5.	Meshing of the NACA 4412 airfoil.	31
3.1.	Validation of NACA simulation for C_l vs α	34
3.2.	Validation of NACA simulation for C_d vs α	34

3.3.	C_l vs α . Blowing velocity at 70 m/s.	37
3.4.	C_l vs α . Blowing velocity at 140 m/s.	38
3.5.	C_d vs α . Blowing velocity at 70 m/s.	38
3.6.	C_d vs α . Blowing velocity at 140 m/s.	39
3.7.	C_l / C_d vs α . Blowing velocity at 70 m/s.....	39
3.8.	C_l / C_d vs α . Blowing velocity at 140 m/s.....	40
3.9.	Velocity profile at 0° for blowing at 70 m/s.	42
3.10.	Velocity profile at 0° for blowing at 140 m/s.	43
3.11.	Velocity profile at 16° for blowing at 70 m/s.	44
3.12.	Velocity profile at 16° for blowing at 140 m/s.	45
3.13.	Velocity profile at 18° for blowing at 70 m/s.	46
3.14.	Velocity profile at 18° for blowing at 140 m/s.	47
3.15.	Velocity profile at 20° for blowing at 70 m/s.	48
3.16.	Velocity profile at 20° for blowing at 140 m/s.	49
3.17.	Velocity profiles, airfoil comparison.....	50

List of Tables:

Table 2.1. Aerodynamic coefficients at different accuracy of the mesh.	29
Table 3.1. Aerodynamic coefficients for NACA 4412.	33
Table 3.2. Aerodynamic coeff. for modification at 0.61c and 70m/s blowing jet.	35
Table 3.3. Aerodynamic coeff. for modification at 0.61c and 140m/s blowing jet. ...	35
Table 3.4. Aerodynamic coeff. for modification at 0.50c and 70m/s blowing jet.	35
Table 3.5. Aerodynamic coeff. for modification at 0.50c and 140m/s blowing jet. ...	36
Table 3.6. Aerodynamic coeff. for modification at 0.39c and 70m/s blowing jet.	36
Table 3.7 Aerodynamic coeff. for modification at 0.39c and 140m/s blowing jet.	36
Table 3.8. Aerodynamic coefficients comparison	37

1. Introduction

This Bachelor Thesis is decomposed in five chapters:

- Chapter 1 is the general introduction to the subject, emphasizing the existing ideas for controlling boundary layer separation. Also, the objectives and hypothesis of this research are stated in this chapter.
- Chapter 2 explains the methodology used for the realization of this study and it is divided in three sections. The first one describes the physics related to the turbulent boundary layer. The second is focused on the selection of the NACA profile of this investigation and its modifications. The third sub-chapter is focused on the CFD set up in ANSYS Fluent to the correct performance of the simulations.
- Chapter 3 shows and discuss the results obtained for the different profiles studied. The data of the aerodynamic coefficients are compared to assist the correct interpretation of the results. Besides, images of the velocity profile at different angles of attack are shown.
- Chapter 4 provides the conclusions of this Bachelor Thesis, as well as future possibilities that this study may open to other investigations.
- Chapter 5 exposes the budget of the project and the legal framework related to the blowing system modification.

1.1 State of the Art and Motivation

From the beginning of the first Wright brothers' flight until nowadays advanced aircraft, aerodynamics and fluid dynamics have been widely studied areas of knowledge. In modern aeronautics, there is one element of incommensurable importance: the boundary layer over a profile.

The boundary layer can be explained as the thin region of fluid which is very close to the solid body surrounded by that fluid, where the effects of frictional viscosity are significant.

The first approach to the boundary layer concept was described by Ludwig Prandtl [1] in 1904 in his paper *Über Flüssigkeitsbewegung bei sehr kleiner Reibung* or *Motion of fluids with very little viscosity*. After Prandtl, a lot of research was conducted by public and private institutions to understand better and to control the boundary layer.

For controlling the boundary layer and improving aerodynamic efficiency, high-lift devices have enormous importance in take-off and landing flight configurations. Procuring a higher lift at high angles of attack allows the aircraft to implement safer manoeuvres. Flaps, slats, blown flaps, leading edge root extensions and Co-Flow Jets are some of the examples of nowadays mechanisms that are designed to increase the amount of lift.

The subject of study of this Bachelor Thesis is the control of the incompressible turbulent boundary layer by means of a blowing modification system: a slot tangential to the surface expels fluid that impedes separation of the boundary layer, producing more lift and delaying stall.

The literature on high-lift devices such as the one of this thesis is little, and most of the works are focused in streams with low Reynolds numbers. Notwithstanding, there have been innovating attempts for controlling the boundary layer that have been patented. Each one of them uses a different idea, with variations of the fluid temperature, viscosity, geometry, porosity, type of fluid injection and quantity of mass flux, among other parameters and other considerations. Hereafter, every investigation has contributed to the state of technique of this Bachelor Thesis.

The original idea of the object of study of this Bachelor Thesis of studying the turbulent boundary layer came from the conceptual modification of a propeller patented by the Spanish inventor Ramón Robles Giménez [2]. He modified the conventional propeller by catching air from an area near the hub and expelling it through a slot near the tip, previous transportation of the air flow by an inner pipe inside the propeller blade. Similarly, the invention created by Barr [3] in 1919 took advantage of the head pressure at the hub (this device would reduce the head resistant of the hub) by conducting the forward air similarly to the Granados-Robles.

Granados-Robles propeller shown in Figure 1.1 is composed by several radial blades, each of them has a longitudinal conduit that leads the air flow taken in the core

section to the final discharge, near the tip, to aid the force in turning the propeller. The remainder of the propeller follows the traditional propeller designs [4].

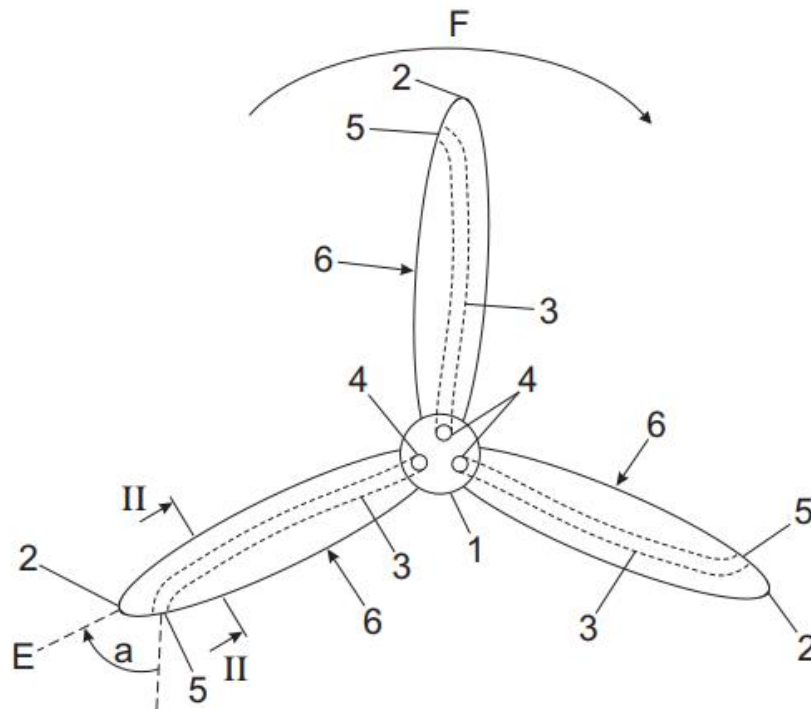


Figure 1.1. Description of Granados-Robles propeller [4, Figure 1].

Similarly, to try to control stall, PhD J. F. Zarate [5] designed a stall reduction propeller with a compressor in the core. The compressor is in charge of generating the airflow which is later expelled through the nozzles for delaying boundary layer separation on the blades. The main difference between Zarate and Robles is that while Zarate wants to control the stalling behaviour, and, for that, he uses the incident flow that goes through the compressor in the core, Robles uses the incident flow to help the thrust (frontal lift) generated with the blades.

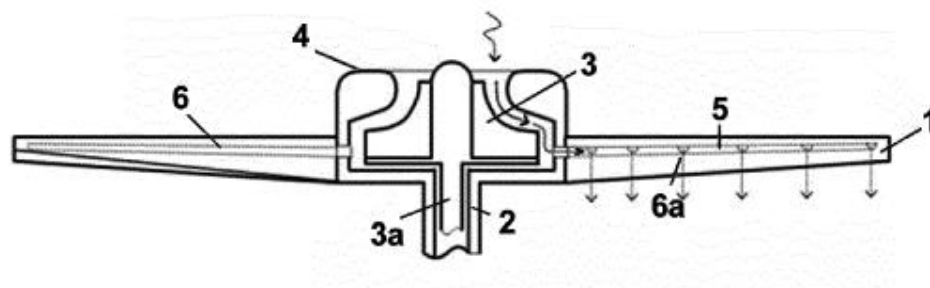


Figure 1.2. Cross-section description of Zarate's propeller [5, Figure 3].

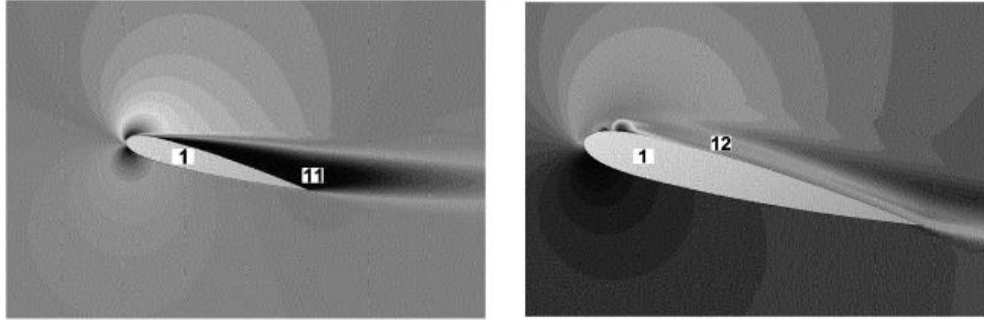


Figure 1.3. Boundary layer of the aerodynamic profile simulated with CFD without the invention (left) and with the invention (right). [5, Figures 6 and 7].

These two inventions are related in the evolution of this Thesis: both are systems that expel fluid, after conducting it internally to avoid or delay the separation of the boundary layer.

Nevertheless, due to the difficulty in studying the strong 3D effects on the flow on the propeller blade, the option of studying the blowing system for boundary layer on propeller's blades escapes from the scope of this Thesis.

Similar concepts have been developed, for example, in high-lift devices where the engine jet exhaust can be blown over the upper surfaces near the leading edges of the wing and trailing edge flaps [6].

High-lift devices can be also seen in nature. The wings of birds like the pigeon *Columba livia* [7] present a boundary layer control system called alula. It works like a slat, controlling the flow on the upper camber of the wing and smoothing the adverse pressure gradients.

Another option to control the flow attached to the surface of the airfoil was considered by Williams [8], who used tangential jet slots at the trailing edge part (Figure 1.4.), to delay detachment of the boundary layer and recover pressure. He claimed that efficiency can be increased, and landing speeds can be reduced due to the higher lift capability of his design.

Four parts can be differentiated in the upper-camber of an airfoil which are referenced in Figure 1.4. as:

- A. Laminar flow area where drag is minimized and maximum lift and thrust happens due to suction. From the leading-edge stagnation point to approximately chord's midpoint.
- B. Instability section right after A; it has a negative slope so adverse pressure gradient appears. Transition from laminar to turbulent flow.
- C. Turbulent flow region with minimum skin friction and likelihood of boundary layer separation.
- D. The trailing edge is like a Coanda profile.

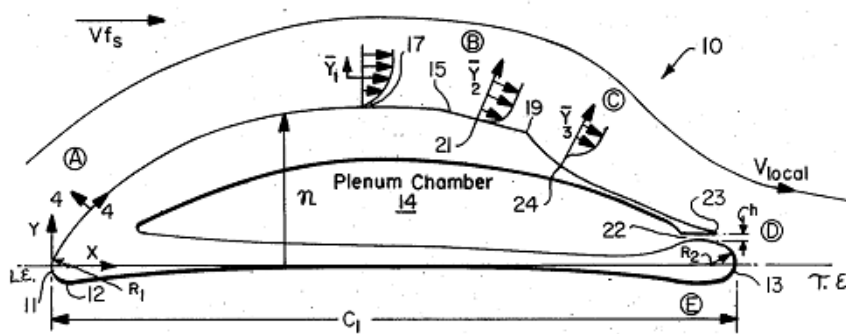


Figure 1.4. Cross-section of the airfoil with Williams' embodiment [8, Figure 1].

This is the reason why, for this thesis, there are 3 positions of the blowing systems to be analysed: at 61%, 50% and 39% of the chord (also expressed as c).

Several research studies and patents have implemented similar ideas for wind turbines or wing section [9]. PhD Sforza [10] employed several embodiments that can be seen in Figure 6. He also recalls in the little existing literature on this subject for the wind turbine case.

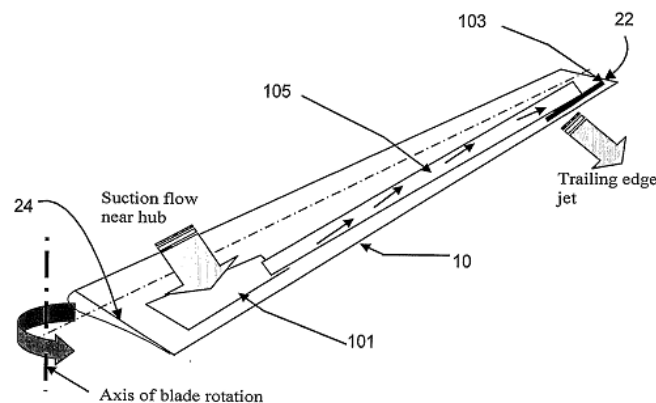


Figure 1.5. Sforza’s blowing system for wind turbines [10, Figure 3].

Academics Ball and Syberg [11] conceived supersonic engine inlets mounted in a way that the inlet receives the blown boundary layer, reenergizing the flow to obtain a high-pressure air source, reducing drag.

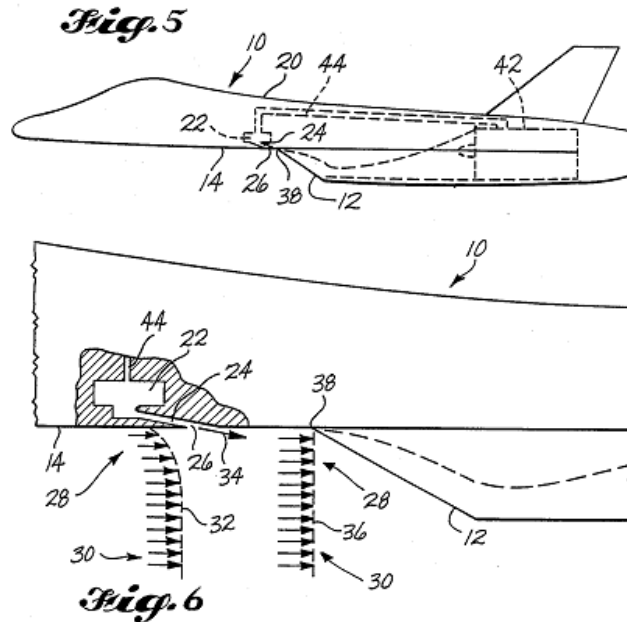


Figure 1.6. Blown boundary layer for supersonic engines [11, Figures 5 and 6].

While there are several ways to control flow separation such as inject air pressurized in a tangential flow direction or vacuum holes to be applied on the boundary layer, Alvi [12] had the idea of microjets to control flow separation (normally due to an adverse pressure gradient) on a surface, as can be observed in Figure 1.7.

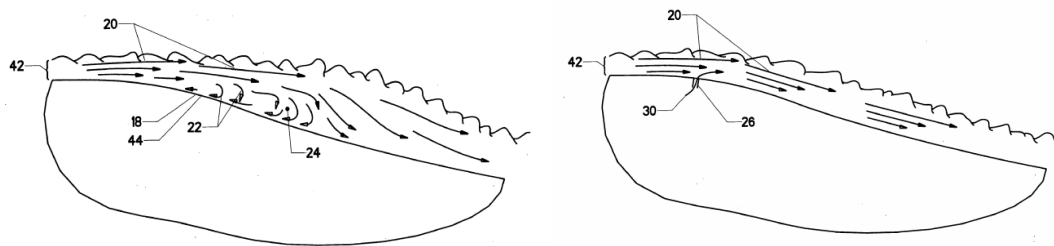


Figure 1.7. Side elevation view, showing a high adverse pressure gradient with detachment of the flow (left) and with the use of microjets (right), delaying separation [12, Figures 3 and 6].

It can be concluded that the flow must be re-energized with a certain amount of mass flow at a certain velocity (Alvi's idea is to use small amounts of air at very high velocities), in a direction transverse to the prevailing flow. From his work, the concept of analysing at different mass flux of the blowing system is taken.

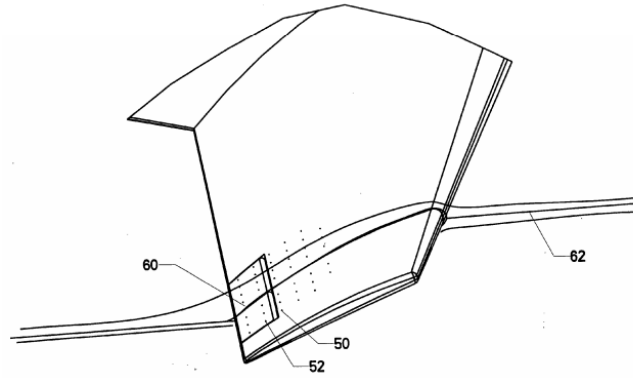


Figure 1.8. Perspective view of a profile with the microjet configuration that preserve non-separated flow [12, Figure 11].

Moreover, further knowledge about wind-turbines possibilities is provided by Bove and Grabau [13] and their lift-regulating device formed of one or more slots or holes that alter the aerodynamic properties of the blade, lowering the load at the hub. Lastly, Campe and Terry [14] created a boundary layer control system with pressure chambers all over the length of the blade, resulting in suction (underpressure area) and blow channel (overpressure area) with an actively operable valve.

1.2 Objectives and hypothesis

All the previous ideas were very useful on valuing the different ways of approaching the boundary layer problem.

The object of study of this Bachelor Thesis is, as stated earlier, the analysis of a high-lift device that controls the boundary layer through an air blowing system over the upper-camber of the airfoil, energizing the air circulation, increasing lift and preventing boundary layer separation. To achieve our goal, several blowing system modifications of the NACA 4412 airfoil are compared with the original profile.

This research could lead to elaborate further investigations for both public and private organizations, serving as an initial step to approach a solution in nowadays aeronautics. This may add several advantages and innovation with respect to other designs, resulting in subsequent benefits to industrial activity, human society and world energetic efficiency.

Kermode [15, p.110] affirms that “on a slotted wing the air flows through the gap in such a way as to keep the airflow smooth, following the contour of the surface of the aerofoil, and continuing to provide lift until a much greater angle is reached. Numerous experiments confirm this conclusion. It is, in effect, a form of boundary layer control.”

Therefore, the idea is to use upper-camber blowing as it is done by a blown or jet flap, or a blown slot, high-lift systems that increase the lift for take-off and landing, and thus, improving the aerodynamic efficiency in these conditions.

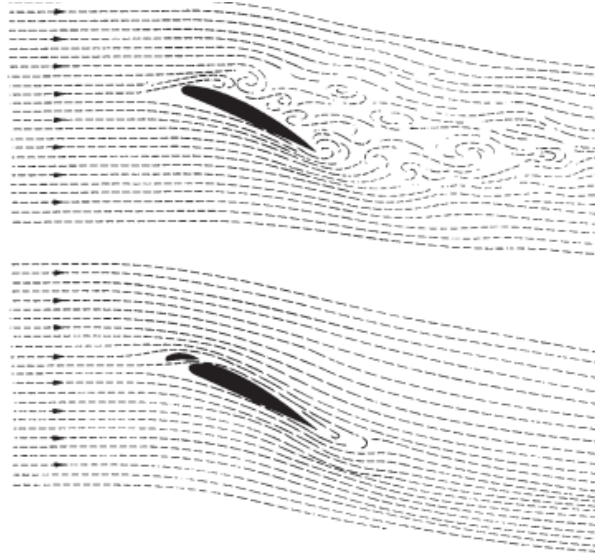


Fig 3.34 Effect of slot on airflow over an aerofoil at large angle of attack

Figure 1.9. Effect of slot on airflow over an aerofoil at large angle of attack [15, Figure 3.34]

The boundary layer blowing system of this research pretends to have a velocity profile as the one shown in Figure 1.10., avoiding the reverse flow and attaching the flow with an increase of velocity in the region of the boundary layer closer to the surface of the body.

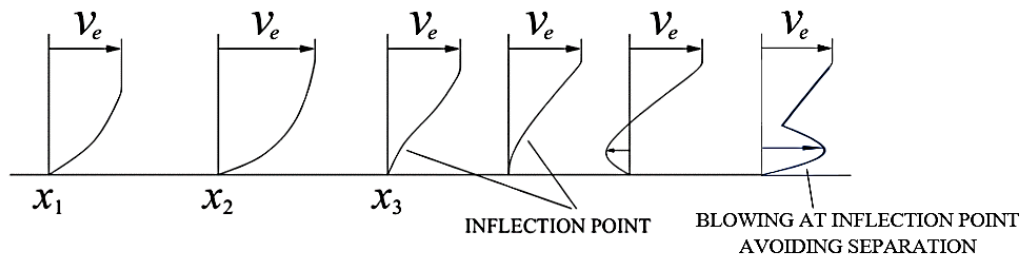


Figure 1.10. Velocity profile of the boundary layer.

With the elaboration of this Thesis about the analysis of a re-energizing blowing system, it is necessary to attain a series of objectives with distinct purposes. The scope of this work is focused on the delay of the 2D boundary layer separation at the upper-camber of a wing profile, since this will result in a further and more complete investigation on the applicability on nowadays aerospace industry.

Therefore, the objectives are:

1. Study the position of the blowing modification.
2. To know the most efficient velocity of the blowing air ejected.
3. To know the changes in aerodynamics with every modification.
4. Move from the conjectures of the patents documented to the demonstration of the suppositions.

In addition, as hypothesis:

1. The detachment of the boundary layer can be avoided or, at least, delayed.
2. The air blown needs a high expelled velocity.
3. The best region of the flow ejection is near the mid-chord.
4. The modification will provide a greater efficiency than the original NACA 4412 airfoil.

One remarkable aspect of this invention is that it could be used not only in airplane wings, but also in propellers (civilian or military), VTOL aircraft, drones or helicopters, but also in wind-turbines, ventilation systems and nautical ships. The innovations that this design would provide may predict efficiency and performance improvements in other fields of application, producing economic benefits.

2. Theoretical background and Methodology

To approach an object of study as complex as the one of this Thesis, it was necessary to review the specialised literature about the matter, as well as experimentation in CFD, in order to obtain reliable and accurate data. The empirical-descriptive method described in the following sub-chapters will explain the theoretical fundamentals and the conditions stated for the correct analysis of the airfoil through several 2D CFD tests.

2.1 Turbulent Boundary Layer

The boundary layer is a narrow and long area in which takes place the molecular transport and convective phenomena with the same importance. It satisfies the boundary condition on the surface of the body that cannot occur in the ideal theory. This area is close to the wall and its thickness is very small compared to its length.

The boundary layer remains attached to the aerodynamic body behaving ideally until the transport phenomena are important. If the body is very long, the boundary layer becomes greater, making invalid the ideal flow theory and creating local pressure losses. Furthermore, if Reynolds number is sufficiently big, the boundary layer can become turbulent, increasing skin friction but also being less prone to separation than in laminar flow (in which fluid particles follow smooth path, with no eddies or swirls that appear in turbulent flow) [16].

Reynolds number (also expressed as Re) is a dimensionless parameter, formed by the ratio of inertial to viscous forces. Reynolds number can be expressed as:

$$Re = \frac{\rho V c}{\mu} \quad (2.1)$$

In the case of this research, at sea level conditions: density $\rho = 1.225 \text{ kg/m}^3$, freestream velocity $V = 70 \text{ m/s}$ and dynamic viscosity $\mu = 1.7895 \cdot 10^{-5} \text{ kg/(m} \cdot \text{s)}$ and chord $c = 1 \text{ m}$. This gives a Reynolds number of $4.8 \cdot 10^6$, which means that the flow can be described as turbulent. In turbulent regimes there is much greater shear at the surface of the body [17].

After seeing the different parts of the upper-camber of an airfoil profile in Chapter 1, it is important to remark that it is desirable a slow gradual deceleration through the point of maximum suction pressure until the trailing edge. Therefore, air flow blowing can be performed near the minimum pressure point on the upper surface.

If this does not occur, the flow will detach since the boundary layer cannot hold the sudden deceleration, resulting into a very complex flow field [18]. This results in higher drag and lower lift, and it can occur at high angles of attack, noticing the high dependence with Reynolds number, Mach number and the own airfoil's shape [19].

The theoretical model leads to acceptable results until the boundary layer is thin and attached, if detachment is produced a wide region of recirculatory fluid with perturbed streamlines appear. This occurs at an inflexion point of separation that loses momentum, since the flow has to deal with the skin friction and the adverse pressure gradient that decelerates the streamlines closer to the wall (in comparison to those that are away from the wall, that have much better conditions to fight this gradient). Thus, the particles close to the wall regress instead of moving forward, detaching the boundary layer. It is in this condition when the viscosity has influence on the pressure field over the airfoil [20].

At the turbulent boundary layer, the exchange of momentum takes place at macroscopic scale, with complex and crisscrossed trajectories, instead of molecular scale at laminar boundary layer. This was noted by Meseguer and Sanz [21], who noted that the flow is rotational on all the turbulent region, while on the main flow far from the boundary layer, the vorticity is null. Hence, it is desirable to counteract the adverse pressure gradient with the injection of an airflow.

Also, a few statements taken by researches about 3D boundary layers need to be considered. For example, Kachanov [22, p. 417] claims that “nonparallel effects can be important for calculating the 3D instability of 2D boundary layers with adverse pressure gradients (including separation), and can explain the more rapid amplification observed for 3D modes, compared with 2D ones. The stability of 3D boundary layers represents a much more complicated case.” This is also important in the transition process with the steady disturbances in 3D.

These last statements unite with Squire [23, p. 628] affirmation: “if any velocity profile is unstable for a particular value of Reynolds’ number, it will be unstable at a lower value of Reynolds’ number for two-dimensional disturbances.” It shows how important is to reach a reliable understanding with the 2D analysis before the studying the 3D flow characteristics, with go in accordance to the comments done by Von Mises [24]. This is one of the reasons of the necessity of this Bachelor Thesis as a proof of concept before a more profound and complete investigation.

2.2 Selection of the NACA profile

For the CFD simulations the airfoil profile needs to be chosen. There are infinitely many profiles that can be used in this Thesis.

After a thorough investigation on the airfoil literature and experiments, the most relevant information was obtained in Sullivan [25] wind tunnel tests of NACA 3414, NACA 8321, NACA 1209, NACA 6217, NACA 0014, and NACA 5417 airfoils; as well as the analysis of NACA 4412 by Kevadiya and Vaidya [26] and the explanatory NACA 6409 and NACA 4412 comparison by Hossian et al. [27].

These investigations showed that the most suitable airfoils for the study of high-lift devices are NACA 4412 and Clark Y, since their behaviour at take-off and landing conditions might be significantly improved with the blowing system of this thesis. In addition to this, an important fact is that leading edge separations result in sudden drop of lift, while in trailing edge separation the loss is more gradual [28]. This is the reason why thicker airfoils with more rounded leading edges tend to delay stall which results in increasing maximum lift.

Furthermore, after a careful consideration, the NACA 4412 was chosen as the airfoil to be analysed. This was due to the much more information, data and researches on the NACA 4412 airfoil than on Clark Y.

The way to prove the hypothesis is by comparing lift and drag coefficients obtained in the computational simulations of the different blowing modifications with the simulation performance of the original NACA 4412.

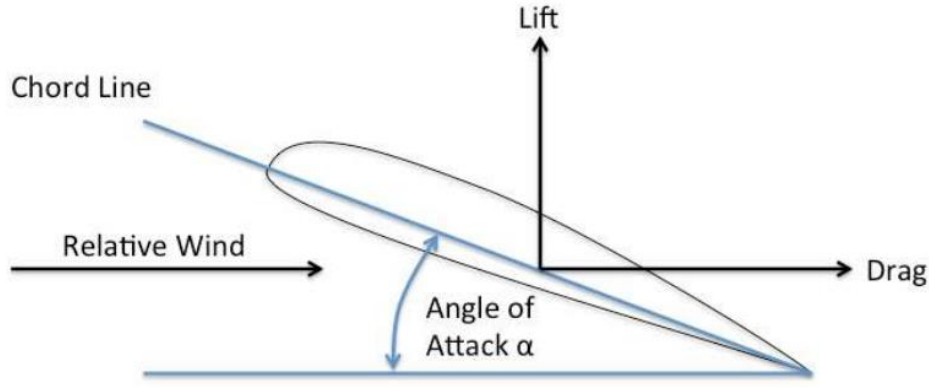


Figure 2.1. Lift, Drag and Angle of Attack on the Airfoil. [41, Figure 1]

Lift coefficient can be expressed as the lift force divided by the dynamic pressure and the area related to the body.

$$C_l = \frac{L}{\frac{1}{2}\rho V^2 A} \quad (2.2)$$

Drag coefficient can be expressed as the drag force divided by the dynamic pressure and the area related to the body.

$$C_d = \frac{D}{\frac{1}{2}\rho V^2 A} \quad (2.3)$$

The profiles created from the NACA 4412 have a chord of 1 metre, a slot height of 1% of the chord and slot location at 61% (first case study), 50% (second case) and 39% (third case). The selection of these three points permits the observation of the blowing effect and helps when deciding the best location of the system. The geometry modification of the NACA 4412 upper camber from the slot location until the trailing edge has the same radius than the original NACA 4412, so the change in geometry is minimum, although noticeable, as it can be observed in Figure 2.2.

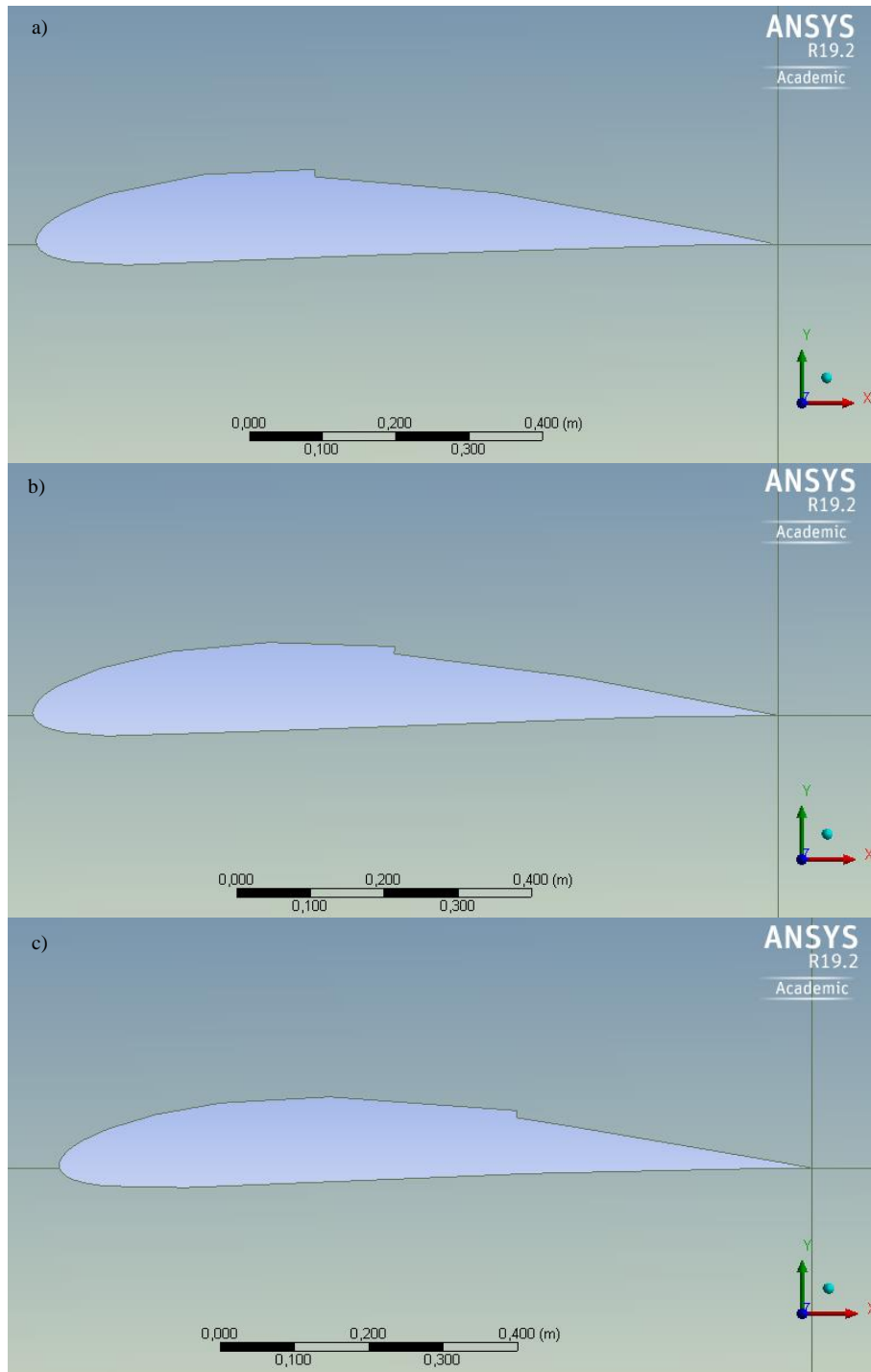


Figure 2.2. Geometry of the modified NACA 4412 with the blowing system.

a) Modification at 0.61 c) Modification at 0.39

2.3 Computational Fluid Dynamics – ANSYS Fluent

The tool chosen to perform the analysis of this Bachelor Thesis is ANSYS Fluent, in its 19.2 version, a Computational fluid dynamics (CFD) software that enables to use both theoretical and experimental in the numerical simulation of complex flow-fields, with fast and thorough strategies when approaching problems of flow analysis.

It is an approach of a huge importance in nowadays fluid dynamics practice since it solves the toughest design challenges with well-validated results in a wide range at distinct conditions (such as inviscid, laminar or turbulent flow over a certain geometry), heat transfer conditions, explicit dynamics or structural analysis with the assistance of numerical analysis, as well as Navier-Stokes equations for compressible and incompressible flows over airfoils [29].

The quick development of CFD allowed faster and more precise strategies for taking care of issues identified with streamlined features. By utilizing ANSYS Fluent, stream examination turns out to be progressively more complete than trial strategy. Nevertheless, the main drawback is that CFD has lack of accuracy in predicting stall.

The geometry designed for the original NACA 4412 and the blowing modifications at 61%, 50% and 39% of the chord were imported to the ANSYS meshing tool.

The CFD analysis was carried out with a density-based solver, using the realizable k - ϵ model with non-equilibrium wall treatment. This model involves the turbulence kinetic energy equation (k) and the dissipation energy equation (ϵ). This is a Reynolds Averaged Navier-Stokes (RANS) turbulence model valid for complex shear flows involving fast strain and transitional flows such as boundary layer separation, since the applicability of non-equilibrium wall function improves the results for flows with higher pressure gradients, separations or reattachment [30]. For this, the value for y^+ , wall adjacent cell centroid, is located within the log-law layer, which means $30 < y^+ < 300$. The solution methods were an implicit formulation and green-gauss cell based gradient option, with second order upwind to discretize the governing equations.

As stated before in this chapter, the air flow was considered as an steady and incompressible fluid at sea-level conditions, with an air-speed at Mach number of $M = 0.205$, density $\rho = 1.225 \text{ kg/m}^3$, temperature $T = 288.16 \text{ K}$ and viscosity $\mu = 1.7895 * 10^{-5} \text{ kg/(m * s)}$, this is an assumption close to reality and, therefore, it is not required to solve the energy equation [31].

At the inlet, turbulence conditions were imposed as turbulence intensity of 0.1% and a turbulence viscosity ratio of 1%, since it is a free flow over an airfoil. The speed of the inlet flow was $V = 70 \text{ m/s}$ with the velocity components obtained with $V_x = V * \cos \alpha$ and $V_y = V * \sin \alpha$, being alpha the angle of attack of the airfoil with respect to the x-axis.

In the case of the slot velocity inlet, the velocity had a direction normal to the slot (tangential to the surface of the airfoil). The chosen jet velocities for the blowing system were 70 m/s and 140 m/s, which means that the amplitude ratio between the blowing jet and the freestream velocity ($A = \frac{V_{jet}}{V}$) are 1 and 2, respectively.

The other imposed boundary conditions were a pressure outlet at the outlet of the domain and no-slip condition at the wall. The domain extended 15c upstream and downstream the airfoil.

To guarantee the right boundary layer modelling, the study of the mesh was carried out. The standard case studied was the unmodified NACA 4412 at angle of attack of 0° . The values obtained for the lift coefficient and drag coefficient were the following:

Nodes	Cl	Cd
3900	0.45144	0.01197
17850	0.43649	0.01031
45360	0.43661	0.01020
57330	0.43684	0.01019
70700	0.43696	0.01019

Table 2.1. Calculated aerodynamic coefficients at different accuracy of the mesh.

From Table 2.1, two comparative curves can be drawn.

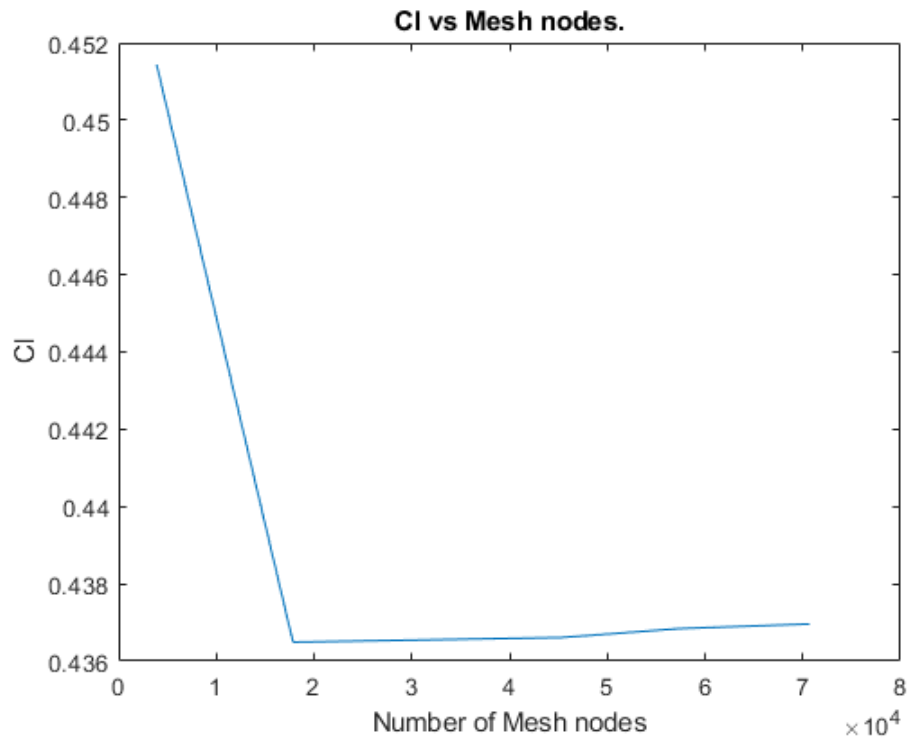


Figure 2.3. Lift coefficient vs number of mesh nodes.

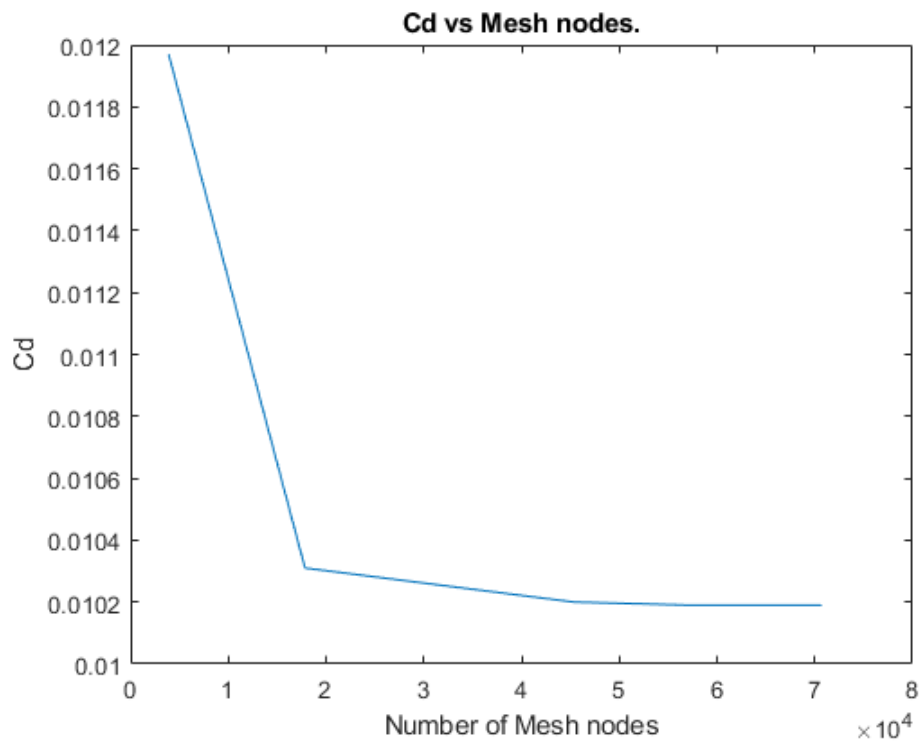


Figure 2.4. Drag coefficient vs number of mesh nodes.

From these results it can be concluded that a mesh with more than 45360 nodes gives accurate and fully reliable values, since a finer mesh would have a greater computational cost [27]. Therefore, the mesh nodes for the airfoils studied are:

- 57330 nodes in the original NACA 4412,
- 56827 nodes in the modified NACA 4412 with blowing at 61% of the chord.
- 51816 in the modified NACA 4412 with blowing at 50% of the chord.
- 54120 in the modified NACA 4412 with blowing at 39% of the chord.

This assumption is also sustained by Rosen [32], who studied the separation regions for various 2D and 3D airfoils and stated that a further refinement of the mesh would have little effect on the velocity profile and on the variation of the aerodynamic coefficients (for 2D airfoils); he claimed also that difference turbulence models predicts the separation point at distinct positions.

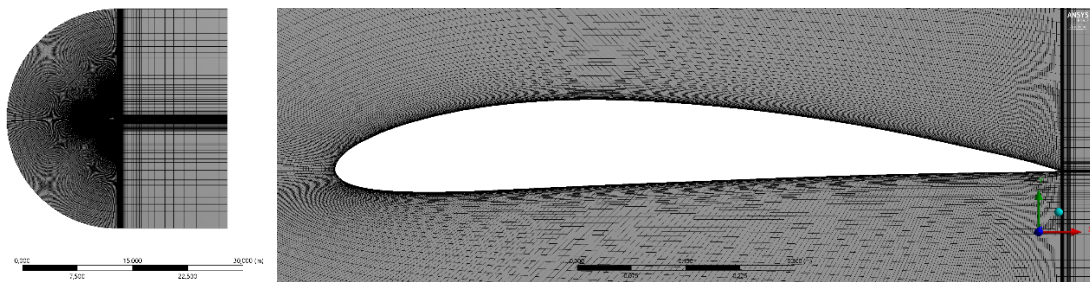


Figure 2.5. Meshing of the NACA 4412 airfoil.

3. Results and Discussion

After the CFD simulations, the results are shown with data tables, comparative graphs and velocity profile images. With these 3 elements, the outcomes of this investigation can be discussed.

3.1 Data

The analysis of the original NACA 4412 airfoil profile gave the following aerodynamic results for the climb range at 70 m/s and 0-20° angle of attack:

Alpha	Cl	Cd	Cl/Cd
0	0.43696	0.01019	42.88126
4	0.85731	0.01370	62.57737
8	1.25952	0.02273	55.41223
12	1.57950	0.03627	43.54839
16	1.76754	0.06262	28.22645
18	1.73763	0.08276	20.99601
20	1.69109	0.11041	15.31646

Table 3.1. Calculated aerodynamic coefficients for NACA 4412.

The results of this thesis are compared to other NACA 4412 tests for turbulent regimes. In the case of the lift coefficient, the first curve represents the experimental wind tunnel test by Wadcock [33] with Reynolds number of 1.64 million, while the second curve shows the work done by Matyushenko et al. [34], with the same conditions that the ones performed in this Bachelor Thesis.

Figure 3.1. shows the evolution of the lift coefficient with the angle of attack. The k- ϵ realizable model of this thesis approached to the experimental case very accurately at pre-separation conditions but failed post-separation conditions if compared to the experimental case. In the experimental case, detachment of the boundary layer occurs at an angle of attack of 12°, while for both experimental cases, it occurs at 16°.

For the drag coefficient in Figure 3.2., since Matyushenko et al. [34] did not studied the drag coefficient for the NACA 4412 airfoil, the data for CFD comparison is taken from the simulation carried out by Petintin and Onoja [35] at Reynolds number of 3 million.

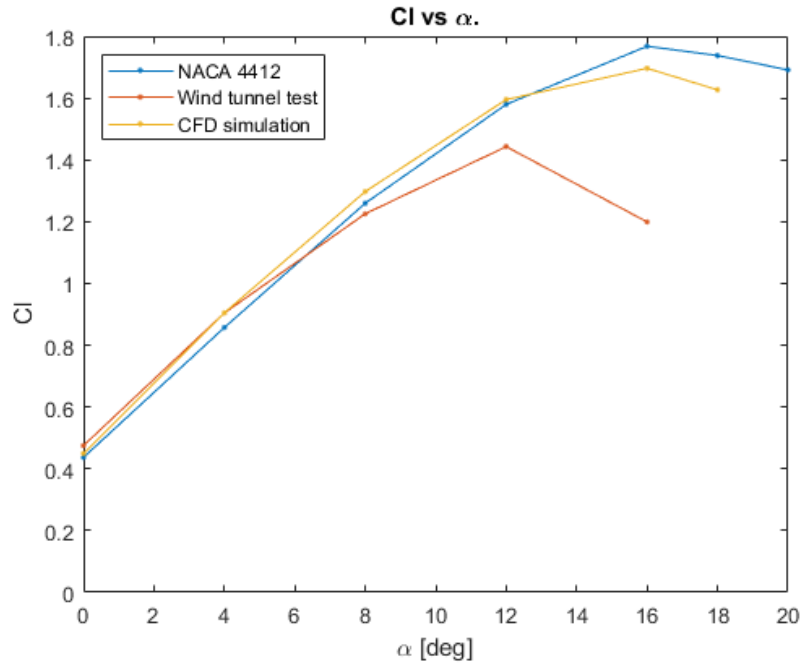


Figure 3.1. Validation of NACA simulation for C_l vs α . The wind tunnel test case is taken from Wadcock [33] and the CFD simulation result is taken from Matyushenko [34].

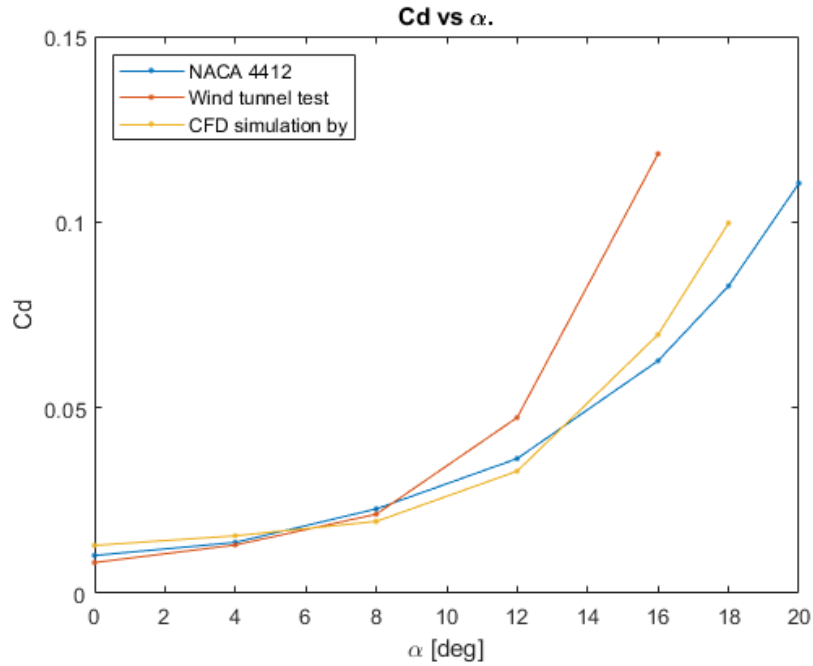


Figure 3.2. Validation of NACA simulation for C_d vs α . The wind tunnel test case is taken from Wadcock [33] and the CFD simulation result is taken from Petinrin and Onoja [35].

Both figures showed that stall occurs at lower angles in the experimental case, while in the CFD analysis separation is delayed, which goes in accordance with what was noted by Yousefi et al. [36].

Afterwards, the modified blowing system for the NACA 4412 was implemented at 61% of the chord. The air blown is expelled at 70 m/s (Table 3.2.), normal to the direction of the blowing slot. Also, the speed at which the air is expelled for blowing was changed to 140 m/s to see the changes in the aerodynamics (Table 3.3.).

Alpha	Cl	Cd	Cl/Cd
0	0.31183	0.00923	35.81782
4	0.72324	0.01173	61.64838
8	1.12361	0.01868	60.15879
12	1.43955	0.03159	45.57241
16	1.75392	0.05790	30.29056
18	1.88315	0.07133	26.40195
20	1.97322	0.09110	21.66100

Table 3.2. Aerodynamic coefficients for modification at 0.61c and 70m/s blowing jet.

Alpha	Cl	Cd	Cl/Cd
0	0.49176	0.01284	40.67356
4	0.96683	0.01715	56.36840
8	1.36548	0.02859	47.75374
12	1.73931	0.04170	41.70897
16	2.06732	0.07348	28.13406
18	2.24618	0.09304	24.14173
20	2.37277	0.11784	20.13574

Table 3.3. Aerodynamic coefficients for modification at 0.61c and 140m/s blowing jet.

The following data for the modified NACA 4412 with blowing system at 50% of the chord was obtained (Table 3.4.). Then, the speed condition of the blowing system was changed to 140 m/s (Table 3.5.).

Alpha	Cl	Cd	Cl/Cd
0	0.28173	0.00958	31.16277
4	0.69664	0.01168	59.6393
8	1.07519	0.01846	58.23763
12	1.39552	0.02968	47.01001
16	1.76278	0.05515	31.96248
18	1.97072	0.07557	26.07857
20	2.04227	0.09644	21.17729

Table 3.4. Aerodynamic coefficients for modification at 0.5c and 70m/s blowing jet.

Alpha	Cl	Cd	Cl/Cd
0	0.51665	0.01450	37.75309
4	1.03444	0.01790	57.78365
8	1.41561	0.02682	52.78637
12	1.78218	0.04144	42.99861
16	2.17150	0.07229	30.03556
18	2.47386	0.09666	25.59216
20	2.57415	0.12356	21.87564

Table 3.5. Aerodynamic coefficients for modification at 0.5c and 140m/s blowing jet.

Finally, the location of the blowing hole was located at 39% of the chord. The results for the 70 m/s blowing speed are shown in Table 3.6. and for the 140 m/s blowing speed the results are shown in Table 3.7.

Alpha	Cl	Cd	Cl/Cd
0	0.24898	0.00904	29.17247
4	0.61009	0.01179	51.73017
8	0.91606	0.01870	48.98080
12	1.22170	0.02997	40.76142
16	1.46245	0.05144	28.42874
18	1.61674	0.07387	21.88619
20	1.69460	0.10453	16.21201

Table 3.6. Aerodynamic coefficients for modification at 0.39c and 70m/s blowing jet.

Alpha	Cl	Cd	Cl/Cd
0	0.486647	0.01387	37.187925
4	0.90554	0.01744	51.92444
8	1.31198	0.02601	50.43728
12	1.64582	0.03987	41.27929
16	2.03580	0.06025	33.78467
18	2.13693	0.08819	24.23218
20	2.24748	0.11630	19.32467

Table 3.7 Aerodynamic coefficients for modification at 0.39c and 140m/s blowing jet.

Likewise, a comparison between the different possible jet velocities for the blowing system was performed at an angle of attack of 16° for the 0.50c modification. Table 3.8. shows that, when increasing velocity, both lift and drag coefficient increase following a similar trend, which results in a variation of efficiency not greater than 9%.

Blowing velocity	Cl	Cd	Cl/Cd
140 m/s	2.17150	0.07229	30.03556
105 m/s	1.94822	0.06151	31.67326
70 m/s	1.76278	0.05515	31.96248
35 m/s	1.56833	0.05317	29.49657

Table 3.8. Aerodynamic coefficients for modification at 0.50c at an angle of attack of 16° .

After obtaining all the data from the analyses in ANSYS Fluent, the comparison of the different profiles is done. For simplicity, each comparison is divided in two plots: the first one for the original NACA and all the blowing configurations at 70 m/s, the second one for the original NACA and all the blowing configurations at 140 m/s.

The first image is the variation of the lift coefficient as function of the angle of attack. In Figure 3.3., it is clear to see how all the modifications at 70 m/s produce less lift than the original NACA 4412 at pre-stall conditions. Notwithstanding, the configurations at 140 m/s produce more lift than the original NACA 4412 at any angle. Also, the modification at 0.5c is the one that has a greater lift coefficient for the 140 m/s.

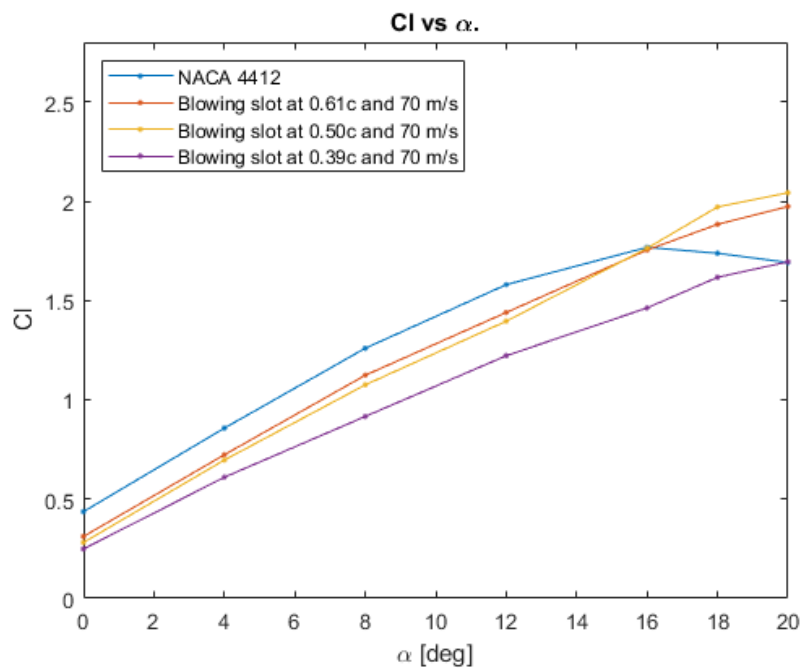


Figure 3.3. Cl vs α . Blowing velocity at 70 m/s.

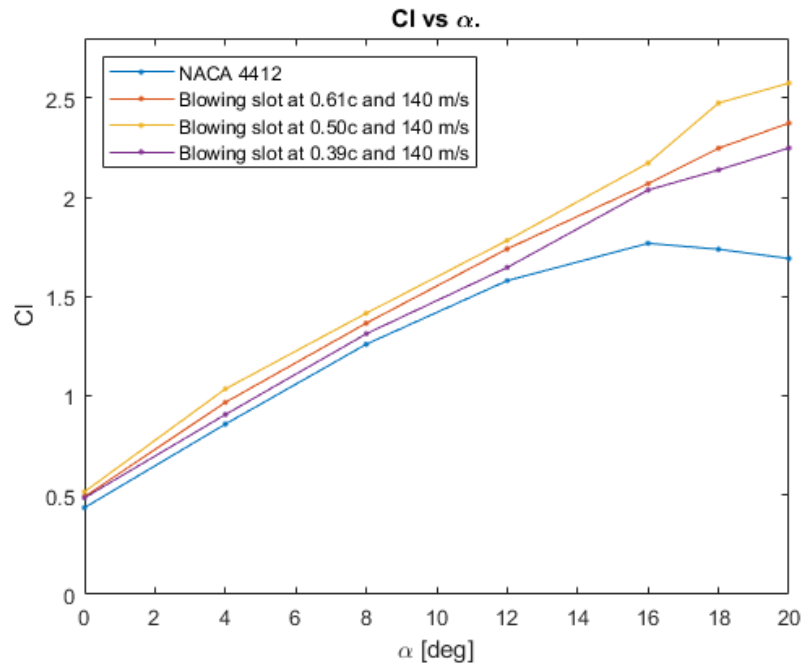


Figure 3.4. C_l vs α . Blowing velocity at 140 m/s.

For the drag coefficient, it is evident that the configuration at 38% of the chord is the best in terms of drag, at both 70 m/s and 140 m/s. However, in all blowing modifications, the use of amplitude ratio of 1 produces lower drag than the original NACA 4412, while for the amplitude ratio of 2, the drag is greater.

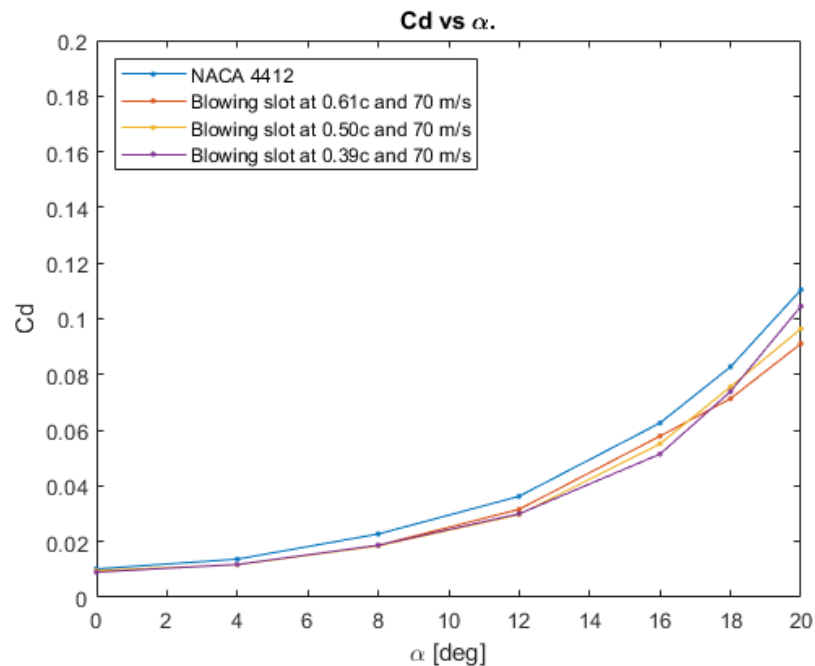


Figure 3.5. C_d vs α . Blowing velocity at 70 m/s.

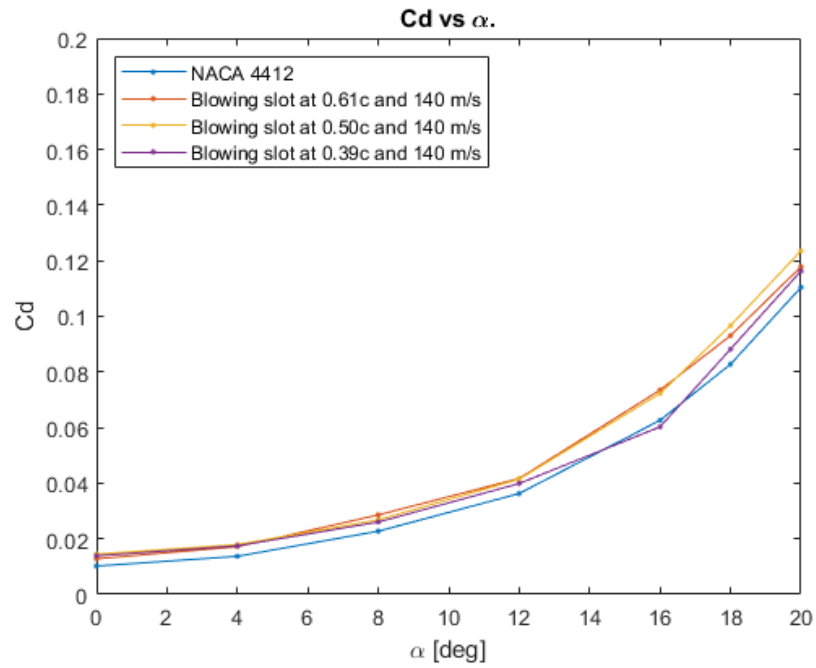


Figure 3.6. C_d vs α . Blowing velocity at 140 m/s.

The aerodynamic efficiency or C_l/C_d is plotted against α to see if there is any change with the modifications designed.

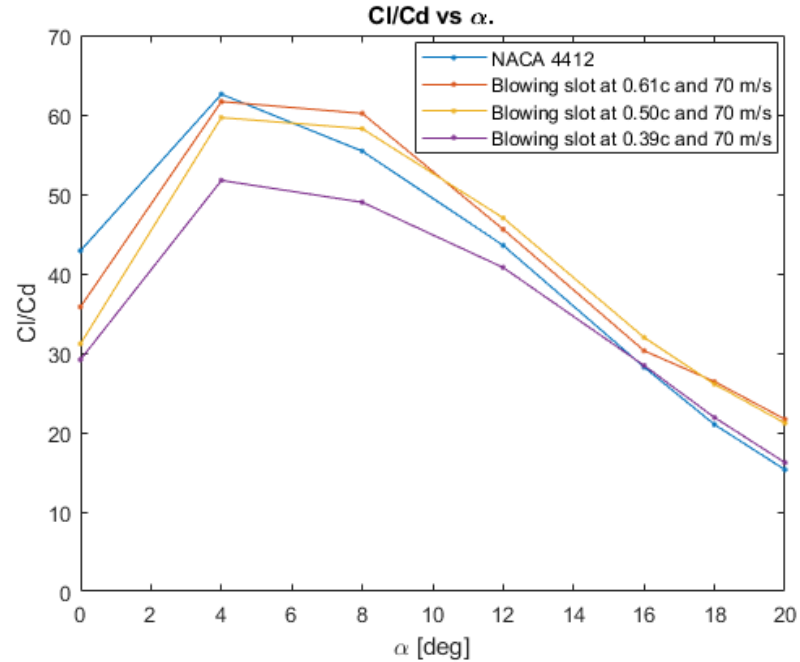


Figure 3.7. C_l/C_d vs α . Blowing velocity at 70 m/s.

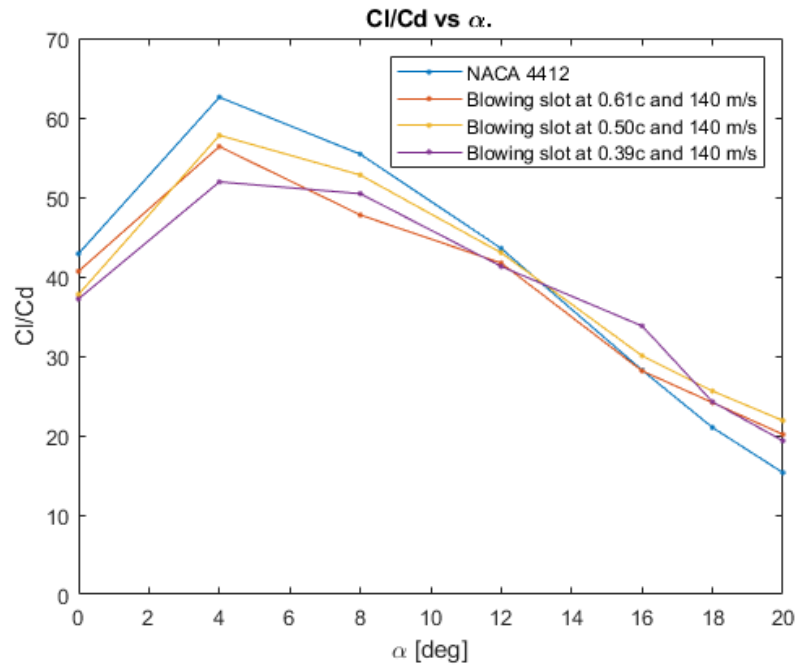


Figure 3.8. Cl/Cd vs α . Blowing velocity at 140 m/s.

From Figure 3.7. and Figure 3.8. and the data from the tables it can be observed that at higher blowing amplitude, the lift-to-drag ratio is increased in the case of the 0.39c modification while at 0.61c the ratio is decreased. For the 0.50c location the variation in aerodynamic efficiency is not that significant. This outcome is noticeable, although the main target is the rise in lift. From these figures it can be stated that the effect at angles lower than 12° the system is unfavourable since Cl/Cd decreases.

3.2 Figures

Besides the data collected, pictures of the velocity profiles were taken to a visual interpretation of what happens at the different embodiments of the blowing system.

Figure 3.9. and Figure 3.10. show the velocity profiles at 0° angle of attack. In these figures it can be observed how the blowing modification of the airfoil interrupts the natural development of the boundary layer.

In Figure 3.09., it can be observed that the flow is expelled at a lower velocity than the one in the NACA 4412, which explains the lower lift coefficient values for 70 m/s. On the other hand, for the case of 140 m/s in Figure 3.10., the flow expelled is at much greater velocity than the flow at the original NACA 4412.

Since the variations in the velocity profiles at high angles of attack are more significant than the variations at low angles of attack, only the results at 16° , 18° and 20° are shown. The following figures show how, at higher angles of attack, the blowing system provides a layer of velocity in a region where the flow normally separates (dark blue area). At an amplitude blowing ratio of 2 (the 140 m/s), the boundary layer remains attached, which allows to generate lift at high angles of attack while the same conditions for unmodified profiles involve stall conditions.

Moreover, Figure 3.17 shows that, at an angle of attack of 16° and modification at 0.50c, with greater blowing jet velocity the boundary layer separation is delayed until it is completely substituted by the blowing jet layer.

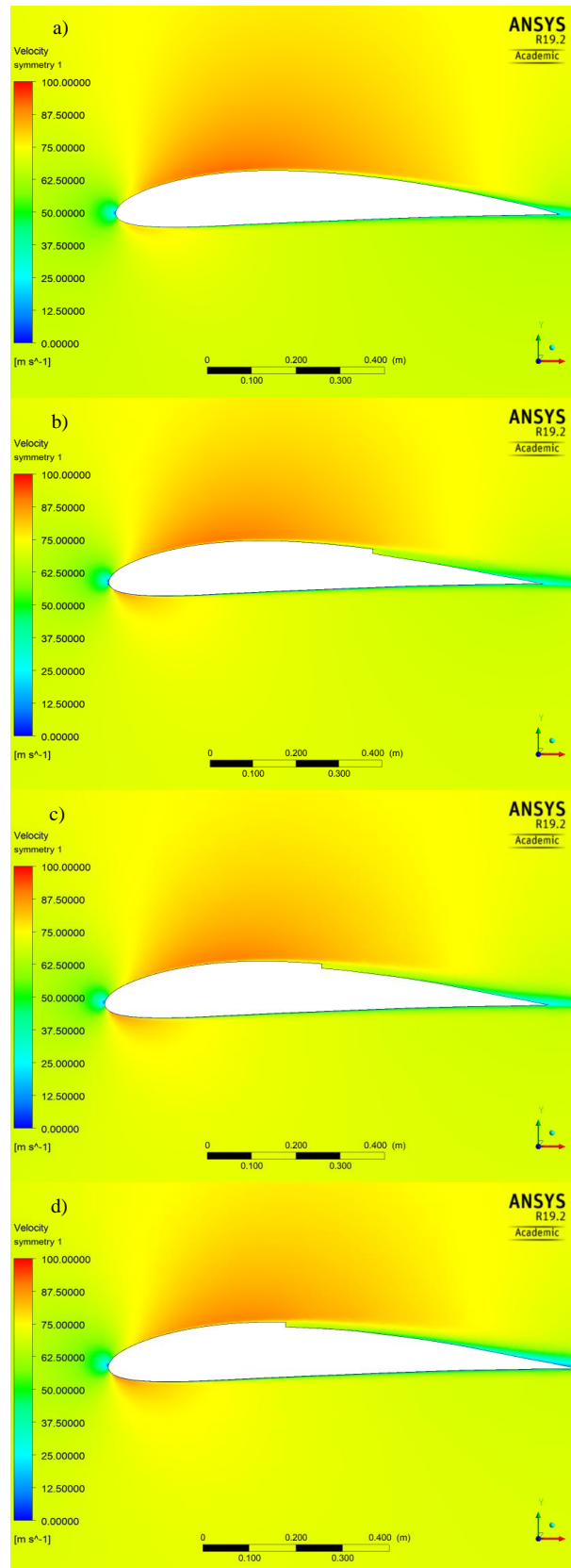


Figure 3.9. Velocity profile of the flow over the airfoil at 0° angle of attack for blowing at 70 m/s.

a) NACA 4412 b) Modification at 0.61. c) Modification at 0.50c d) Modification at 0.39c

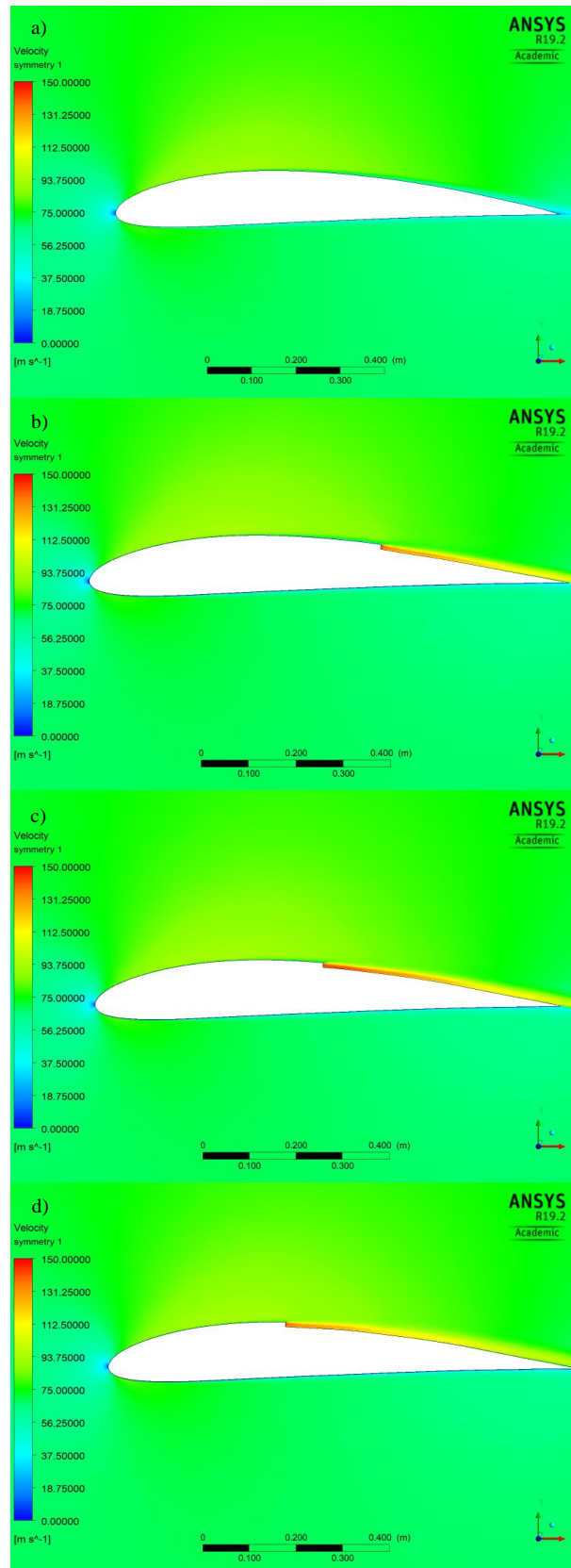


Figure 3.10. Velocity profile of the flow over the airfoil at 0° angle of attack for blowing at 140 m/s.

a) NACA 4412 b) Modification at 0.61c c) Modification at 0.50c d) Modification at 0.39c

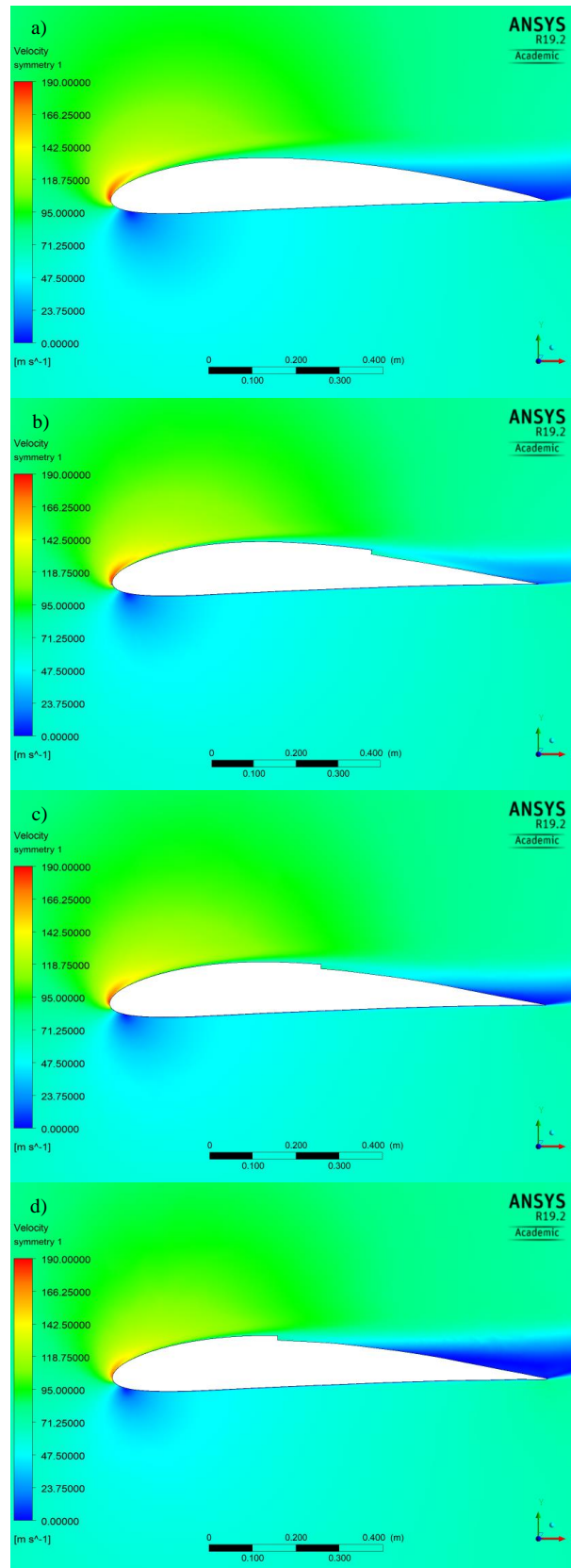


Figure 3.11. Velocity profile of the flow over the airfoil at 16° angle of attack for blowing at 70 m/s.

a) NACA 4412 b) Modification at 0.61 c) Modification at 0.50 d) Modification at 0.39

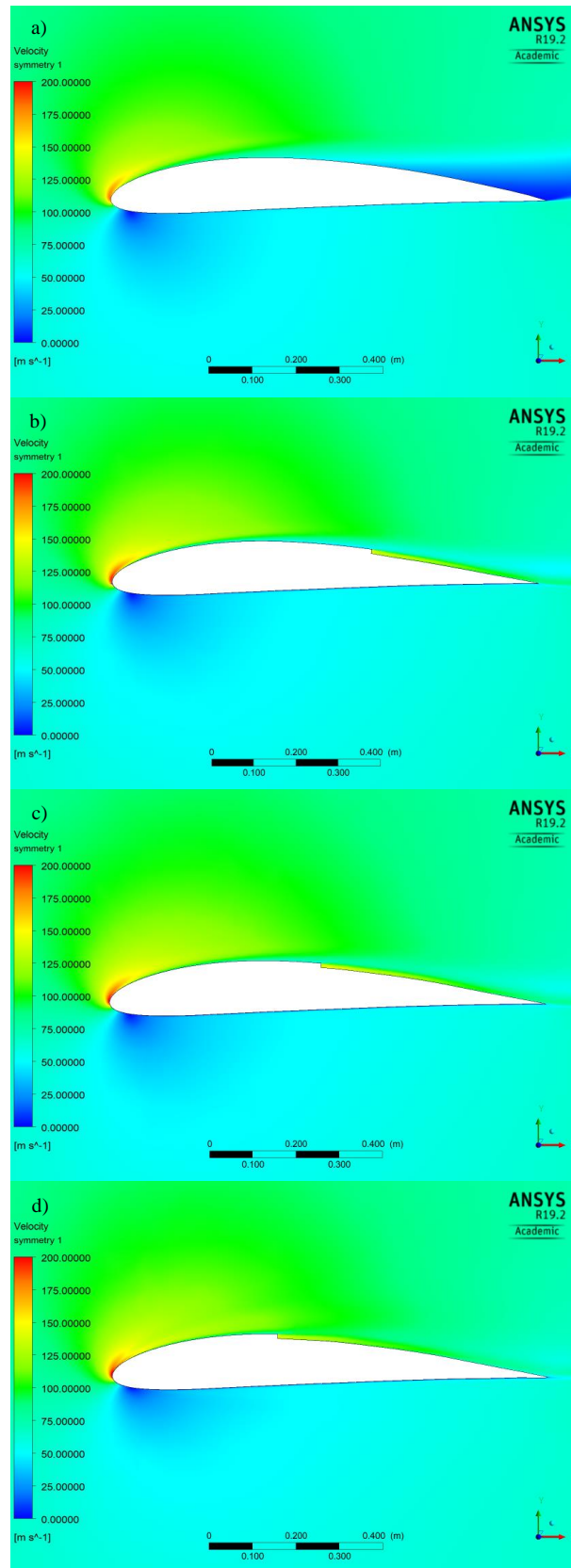


Figure 3.12. Velocity profile of the flow over the airfoil at 16° angle of attack for blowing at 140 m/s.

a) NACA 4412 b) Modification at 0.61c c) Modification at 0.50c d) Modification at 0.39c

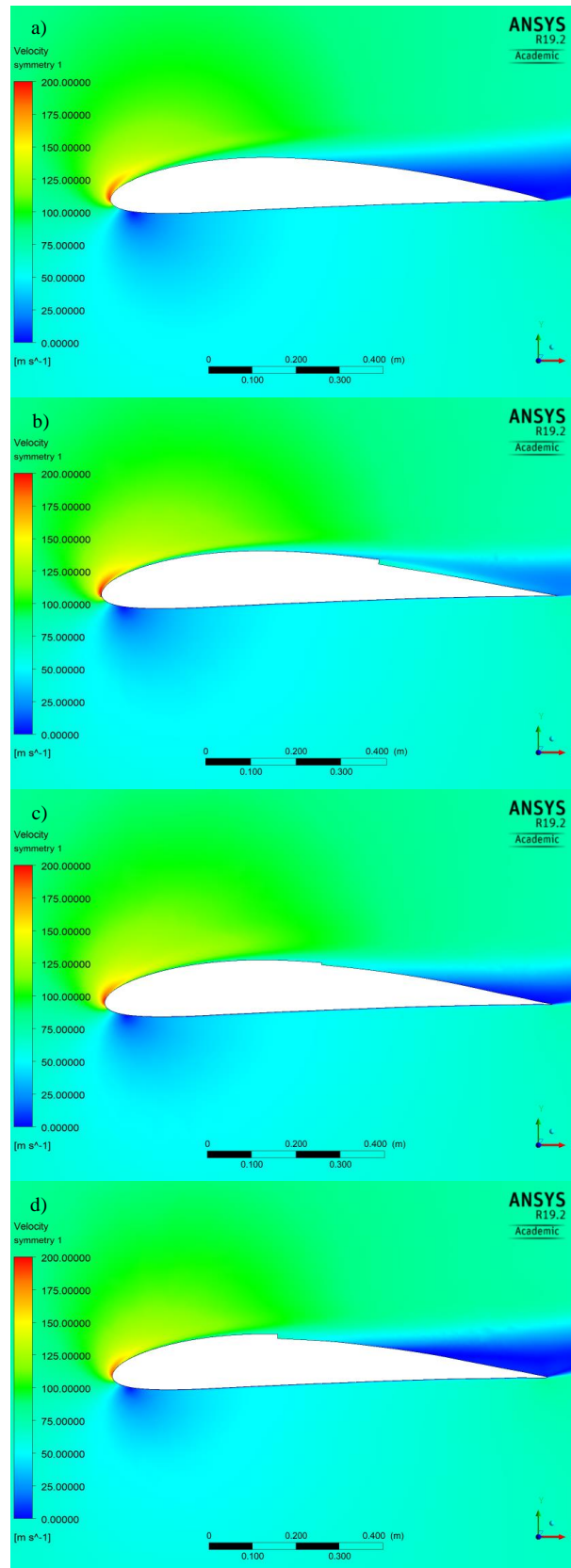


Figure 3.13. Velocity profile of the flow over the airfoil at 18° angle of attack for blowing at 70 m/s.

a) NACA 4412 b) Modification at 0.61c c) Modification at 0.50c d) Modification at 0.39c

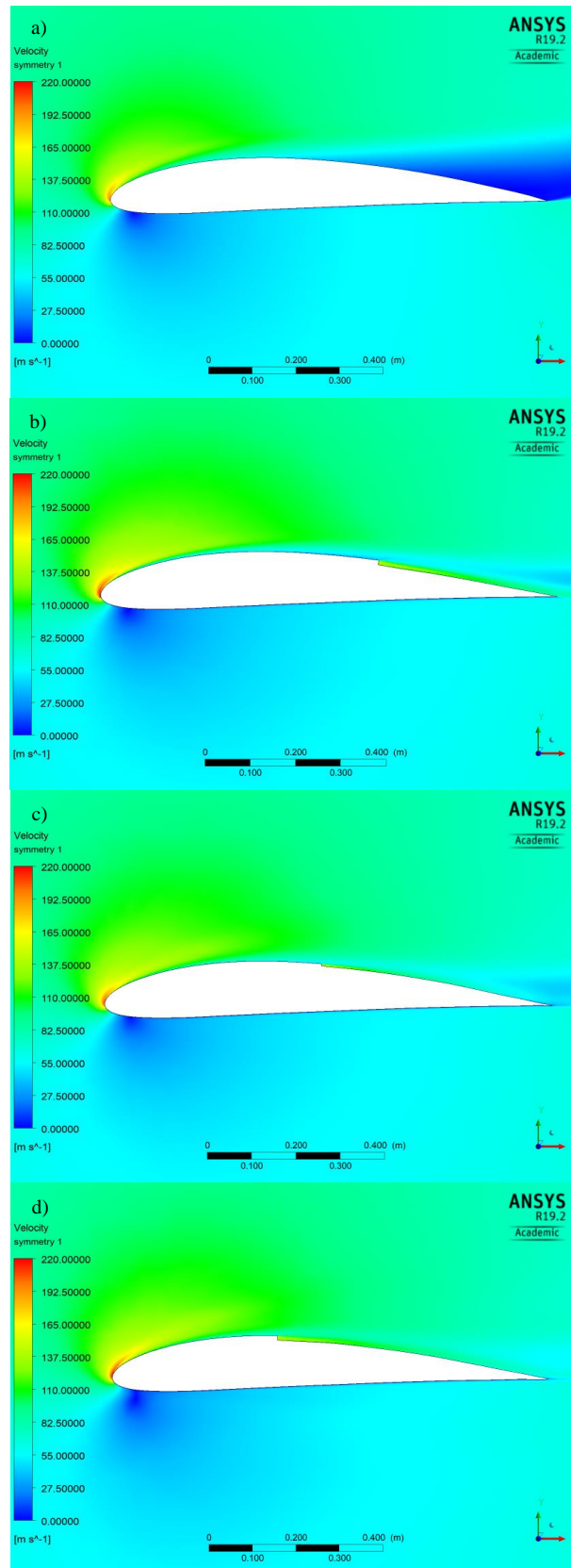


Figure 3.14. Velocity profile of the flow over the airfoil at 18° angle of attack for blowing at 140 m/s .

a) NACA 4412 b) Modification at 0.61c c) Modification at 0.50c d) Modification at 0.39c

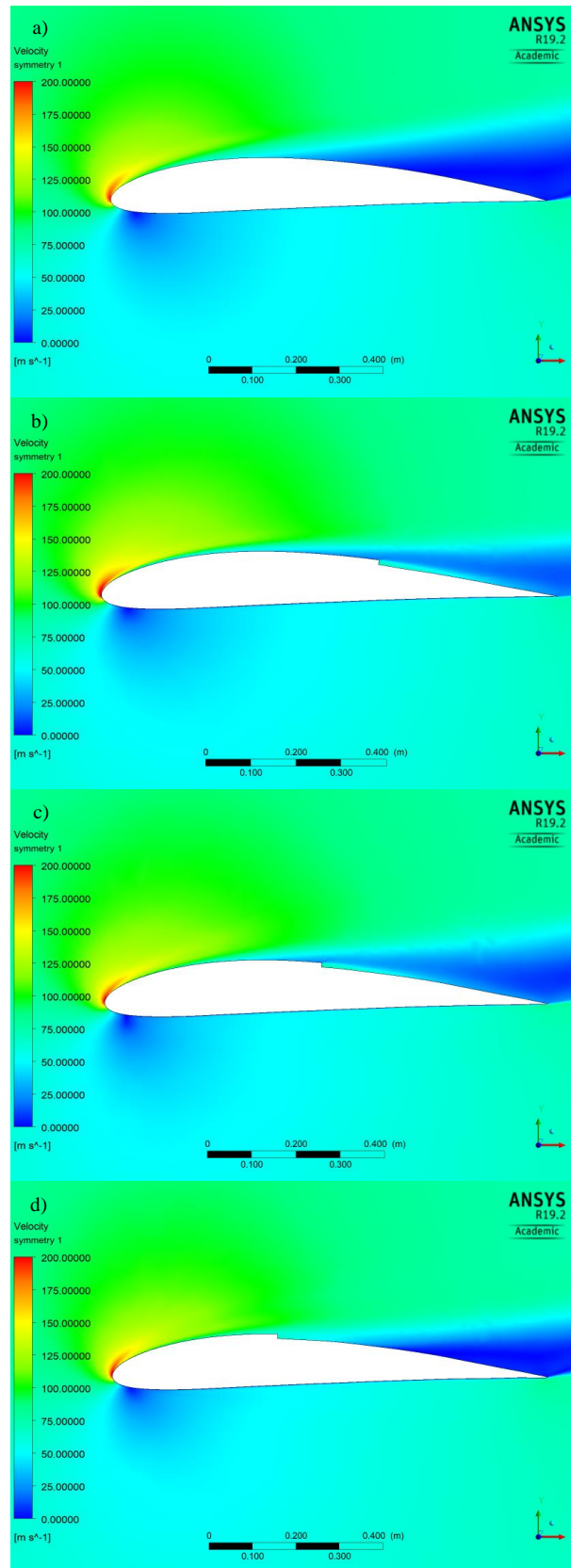


Figure 3.15. Velocity profile of the flow over the airfoil at 20° angle of attack for blowing at 70 m/s.

a) NACA 4412 b) Modification at 0.61 c) Modification at 0.50 d) Modification at 0.39

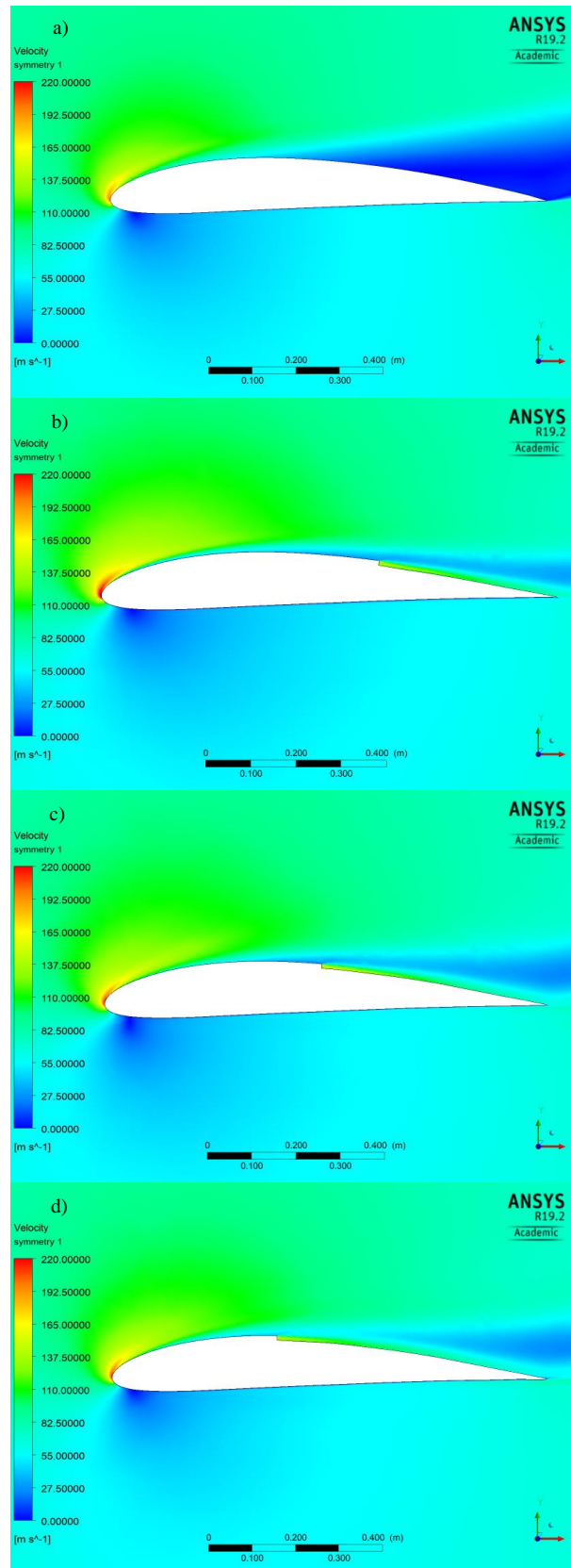


Figure 3.16. Velocity profile of the flow over the airfoil at 20° angle of attack for blowing at 140 m/s.

a) NACA 4412 b) Modification at 0.61 c) Modification at 0.50 d) Modification at 0.39

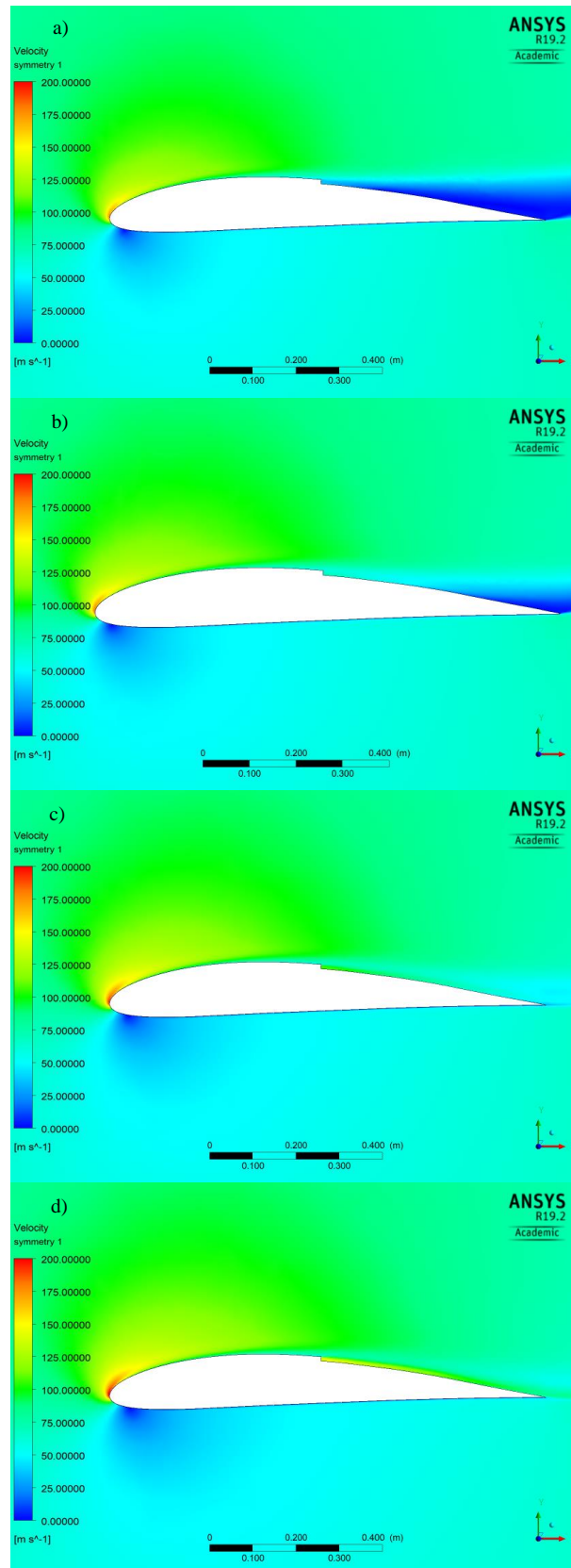


Figure 3.17. Velocity profiles comparison for the airfoil with blowing system at $0.50c$ with 16° angle of attack. The velocities of the blowing jet are the following: a) 35 m/s b) 70 m/s c) 105 m/s d) 140 m/

4. Conclusions

The results obtained with ANSYS Fluent agree with experimental data in the case of attached flow. Notwithstanding, when separation occurs, the values obtained in the simulation for C_l are greater than in the experimental cases [33]

For the differences in the values of the results obtained, the comments of Matyushenko et al. [34] are considered. They studied this lack of accuracy for incompressible turbulent boundary layer regime (reaching 40% of deviation in some papers) and found out that this great difference was not due to neither the test section height of the wind tunnel in the experimental results, the influence of flow compressibility nor the change in RANS turbulent model. Hence, what seems to be the cause of this divergence is the 3D character of the airfoil tested at the wind tunnel, while in the computational simulations it is in 2D. In addition to this, it is possible that all the turbulence models are having a common flaw with overestimating the C_l when detachment appears, failing when locating the separation point and the evolution from laminar to turbulent regime [32]. This imprecision appears in drag coefficient estimation between computational and experimental results at high angles of attack, with any turbulence model used [37].

Another point of interest is the aerodynamic efficiency. Considering the curves from the original NACA 4412 and the modifications for the blowing system created, all of them follow a valid approach that is in the range to the work done by Jiao and Lu [38].

The modified airfoil with blowing system at 50% of the chord has demonstrated to be the one with the greater lift and better efficiency than any of the other possibilities.

Thus, it is more aerodynamically efficient and can allow the airplane to operate at lower take-off velocities. In fact, the differences with the original NACA 4412 in terms of percentage can be observed in Table 4.1 and Table 4.2

Alpha	C_l	C_d	C_l/C_d
12	-11.65%	-18.15%	7.95%
16	-0.27%	-11.93%	13.24%
18	13.41%	-8.69%	24.21%
20	20.77%	-12.65%	38.26%

Table 4.1. Variation of the modified NACA 4412 at 50% of the chord and 70 m/s with respect to the original NACA 4412 airfoil.

Alpha	Cl	Cd	Cl/Cd
12	12.83%	14.27%	-1.26%
16	22.85%	15.44%	6.39%
18	42.37%	16.80%	21.89%
20	52.22%	11.91%	42.82%

Table 4.2. Variation of the modified NACA 4412 at 50% of the chord and 140 m/s with respect to the original NACA 4412 airfoil.

The project successfully accomplished the objectives 1, 3 and 4 stated in Chapter 1, since the location of the blowing modification was studied, as well as the aerodynamic coefficients of these distinct points. However, for objective 2 further research is needed if the most efficient velocity wants to be found.

Moreover, hypothesis 1, 2, and 3 are proved to be correct. Firstly, boundary layer separation was delayed in some cases and completely avoided in others. Secondly, for boundary layer to be attached a high jet blowing is needed. Lastly, the best location for obtaining greater lift and be more aerodynamically efficient is the mid-chord position.

For hypothesis 4, the modification shows indeed greater efficiency than the original NACA 4412, but only at high angles of attack, $\alpha < 16^\circ$, for the case of 140 m/s of blowing speed. For the case of 70 m/s of blowing speed only modifications at 0.50c and 0.61c have better aerodynamic efficiency at angles $\alpha < 8^\circ$.

A possible drawback of the high-lift device by blowing system is that the energy consumption of this process would be too high to be implemented, looking at the estimation of the balance between the consumed power and the lift gained with the system. [39].

Also, the supply of the pressurized fluid is one of the considerations derived from this research. For example, it might be provided by an independent compressor onboard (with the penalty of increasing the weight of the aircraft) or from the engine (that would not be available in case of engine failure). However, it is not a topic of this Thesis and it should be studied accordingly to the power requirement and structural and dependency limitations.

Further works may focus in wind tunnel testing of this system, as well as its 3D analysis. Since the majority of the investigations of high-lift devices by blowing have been performed with low Reynolds numbers, it is encouraged to study the flow at high Reynolds number regimes. Even at supersonic regimes, micro jet blowing systems are useful for turbulent boundary layer control [40]. Other relevant parameter for the control of the boundary layer should be studied, such as slot arrangements, changes in geometry of the airfoil and differences in blowing jet velocity.

5. Socio-economic context and Regulatory framework

The socio-economic framework of this investigation's set up is a proposed budget for the associated costs of this Bachelor Thesis. It is going to be estimated for two cases, the case of an engineer with a full-time position and the case of an intern in a company. It can be decomposed in the succeeding way:

Engineer salary. This research can be performed by an engineer that can have a full-time job or an internship. The reference taken for full-time position was the “XVIII convenio colectivo nacional de empresas de ingeniería y oficinas de estudios técnicos”, that stated that the minimum gross wage for junior engineers is 17,544.24 €/year. This salary is divided by the maximum number of working hours of 1800, which results in 9.75 €/hour. Considering that the total number of hours employed for this investigation was 400 hours, the labour costs are 3,900 €.

Since internship wages depend on the company more widely than full-time position, the reference taken was the SMI (gross interprofessional minimum salary) of 2019 of 12,600 €/year, since it is legislated according to “Real Decreto 1462/2018, de 21 de diciembre, por el que se fija el salario mínimo interprofesional para 2019.”, resulting in 7 €/hour. For the 400 hours of this project, the labour costs are 2,800 € (without taking into consideration the fiscal benefits for the company of having this kind of employee).

Software systems. The software used for the CFD analysis was ANSYS Fluent. License pricing depends whether the user is a private company or if the user is a student performing an academic investigation in a company. It also depends on the package and time of use of the license. The price for the needed 1-year ANSYS Academic Associate licence is 16,500 €, while the price for a commercial license is 36,390 €.

Equipment. The performance must be carried out in a computer or laptop that is able to use ANSYS Fluent software. The estimated price of a computer that fulfils, at least, such requirements is 800€. This computer also has a Windows 10 operative system and Microsoft Office Package.

Electricity. A reasonable cost of the computer energy consumption is 50€ for the duration of this project.

The total final costs are 20,150€ in the case of a curricular internship and 41.410€ in the case of a full-time position. The following table sums up the budget.

Category	Internship	Full-time
Salary	2,800 €	3,900 €
Software	16,500 €	36,390 €
Equipment	800 €	800 €
Electricity	50 €	50 €
Total cost	20,150 €	41,140€

Table. Budget of the project.

As stated previously, it is proved that the implementation of this blowing could provide higher efficiency, reducing fuel consumption and the costs per flight. If the profit margin of the companies increases thanks to this device, the economic benefits can be an incentive to more investigations related to the topic of a blowing system for controlling the boundary layer not only in the aeronautical field, but also in car, train and boat industries.

The reduction of fuel consumption results in less emissions, which follows the trend marked by the Advisory Council for Aeronautical Research in Europe (ACARE).

This study may have the opportunity of being a patentability object as a utility model, since it is an upgrade of invented systems, but it has the peculiarity that its particular design has not been analysed or patented before this Bachelor Thesis: a blowing slot that uniformly expels air conducted internally through the wing, temporarily modifying the geometry of that wing only when it is being used.

The system studied in this investigation is considered a Utility Model according to “Ley 24/2015, de 24 de julio, de Patentes”, since it shows the requirements of Articles 4, 6, 8 and 9, as a possible industrial application after an innovative inventive activity. The patent will adjust to the specific norms and rules of the Spanish Patents Office “Oficina Española de Patentes y Marcas”.

In case of implementation of the high-lift device of this thesis in aircrafts, the Certification Specifications (CS) for European aircrafts (published by the European Aviation Safety Agency or EASA) must be followed. In case of civil transport aircrafts heavier than 5670 kg, the design standards and methods to compliance are set out in CS-25 mandatory regulations. In case of applicability in European military aircraft, the NATO Standardization Agreements must be fulfilled.

References

- [1] L. Prandtl, “Über Flüssigkeitsbewegung bei sehr kleiner Reibung”, 3rd Intern. Math. Kongr. Heidelberg, 1904. pp. 484–491. (Transl. as “Motion of fluids with very little viscosity”, NACA-TM 452).
- [2] R. Robles Giménez, “Hélice”, Spain Patent ES1058948U, 1st of March, 2005.
- [3] L. Barr, “Airplane-Propeller”, United States of America Patent US1300552A, 15th of April, 1919.
- [4] R. Robles Giménez, “Hélice”, Spain Patent ES2569724A2, 12th of December, 2016.
- [5] J.F. Zarate Araiza, “Stall reduction propeller”, Spain Patent ES3064431A1, 7th of September, 2016.
- [6] L.T. Goddmanson and L. B. Gratzner. "Recent advances in aerodynamics for transport aircraft", 9th Annual Meeting and Technical Display, Washington DC, 1973. **[Online]. Available at:** <https://doi.org/10.2514/6.1973-9>
- [7] J. Meseguer, J.C. Álvarez, and A. Pérez, “Formas de retrasar la entrada en pérdida en las alas de las aves”, Instituto Universitario de Microgravedad, Universidad Politécnica de Madrid, Madrid, Spain, 2004 **[Online]. Available:** <http://www.actiweb.es/seosierradegadarrama/archivo2.pdf>
- [8] R. Williams, “Minimum drag circulation profile”, United States of America Patent US37565401A, 4th of September, 1973.
- [9] 이정상, 김기현, and 유철. 최상민, “Blade for wind power generating system and power generating systems using same”, South Korea Patent WO2011159091A2, 22nd of December, 2011.
- [10] P. Sforza, “Wind turbine blade comprising a boundary layer control system”, United States of America Patent WO2007035758A, 29th of March, 2007.
- [11] W.H. Ball, and J. Syberg, “Apparatus for re-energizing boundary layer air”, United States of America Patent US4749151A, 7th of June, 1988.

-
- [12] F. Alvi, “Method of using microjet actuators for the control of flow separation and distortion”, United States of America Patent US20090261206A1, 22nd of October, 2009.
- [13] S. Bove, and P. Grabau, “Wind turbine blade with lift-regulating means in form of slots or holes”, United States of America Patent US20100014970A1, 21st of January, 2010.
- [14] R. Campe, and E. Terry, “Wind turbine with boundary layer control”, United States of America Patent US20100266382A1, 21st of October, 2010.
- [15] A.C. Kermode, *Mechanics of Flight*. 11th ed. Harlow: Pearson, 2006
- [16] A. Crespo Martínez. *Mecánica de Fluidos*, 1st ed. Madrid: Ediciones Paraninfo, 2006.
- [17] L. D. Landau, and E. M. Lifshitz, *Mecánica de Fluidos*, 1st ed. Madrid: Editorial Reverté, 1991.
- [18] J.D. Anderson, “Ludwig Prandtl's boundary layer”, *Physics Today*, 12, 58, pp. 42-48, December 2005. **[Online]. Available at:** <https://doi.org/10.1063/1.2169443> **Accessed:** January 2019.
- [19] W. Johnson, *Helicopter theory*, 6th ed. New York: Dover Publications, 1994.
- [20] J.D. Anderson. *Fundamental of Aerodynamics*. 5th ed. New York: McGraw-Hill, 2011
- [21] J. Meseguer Ruiz, and A. Sanz Andrés, *Aerodinámica Básica*. 2nd ed. Madrid: Garceta Grupo Editorial, 2010.
- [22] Y. Kachanov, “Physical Mechanisms of Laminar-Boundary-Layer Transition”, *Annual Review of Fluid Mechanics*, vol. 26. pp. 411-482, November 2003 **[Online] Available:** <https://doi.org/10.1146/annurev.fl.26.010194.002211> **Accessed:** March 2019.
- [23] H.B. Squire, "On the Stability for Three-Dimensional Disturbances of Viscous Fluid Flow between Parallel Walls", *Proceedings of the Royal Society of London. Series A, Containing Papers of a Mathematical and Physical Character*, vol 142, no. 621-628, 1933. **[Online] Available:** <https://doi.org/10.1098/rspa.1933.0193> **Accessed:** March 2019.
- [24] R. Von Mises, W. Prager, G. Kuerti and K.H. Hohenemser, *Theory of Flight*. 1st ed. New York: Dover Publications, 1959.

-
- [25] A. Sullivan, “Aerodynamic forces acting on an airfoil”, Physics Department, The College of Wooster, Ohio, United States of America, 2010. **[Online] Available:** http://physics.wooster.edu/JrIS/Files/Sullivan_Web_Article.pdf
- [26] M. Kevadiya, and H. Vaidya, “2D Analysis of NACA 4412 Airfoil.” *International Journal of Innovative Research in Science, Engineering and Technology*, vol. 2, no. 5, pp. 1686 -1691, May 2013. **[Online] Available:** http://www.ijirset.com/upload/may/57_2D%20ANALYSIS.pdf
- [27] M.D.S. Hossain, M. F. Raiyan, M.N.U. Akanda, and N.H. Jony, “A Comparative Flow Analysis of NACA 6409 and NACA 4412 Aerofoil”, *International Journal of Research in Engineering and Technology*, vol. 3, pp. 342-350, 2014. **[Online] Available:** <https://doi.org/10.15623/ijret.2014.0310055> **Accessed:** February 2019.
- [28] B. McCormick, *Aerodynamics, aeronautics and flight mechanics*, 2nd ed. Hoboken (New Jersey): Wiley, 1995.
- [29] J.D. Anderson, *Computational Fluid Dynamics.: The Basics with Applications*. Department of Aerospace Engineering. University of Maryland. 1st ed. McGraw-Hill.
- [30] ANSYS Inc, *Modeling Turbulent Flows. Introductory FLUENT Training*, 2006 **Accessed:** March 2019. **[Online] Available:** http://www.southampton.ac.uk/~nwb/lectures/GoodPracticeCFD/Articles/Turbulence_Notes_Fluent-v6.3.06.pdf
- [31] T. Ahmed, T Amin, S.M.R. Islam, and S. Ahmed, “Computational study of flow around a NACA 0012 wing flapped at different flap angles with varying Mach numbers.” *Global Journal of Researches in Engineering*, vol 13, no. 4, pp. 4-16, 2013.
- [32] A.M. Rosen, “Turbulence Modeling for Subsonic Separated Flows Over 2-D Airfoils and 3-D Wings.” **Master Thesis**, Department of Aeronautics and Astronautics, Purdue University, West Lafayette, United States of America, 2013. **[Online] Available:** https://docs.lib.purdue.edu/open_access_theses/121
- [33] A.J. Wadcock, “Investigation of low-speed turbulent separated flow around airfoils”, National Aeronautics and Space Administration, United States of America, Contractor Report NAS2-11601, 1987.

-
- [34] A.A. Matyushenko, V.E. Kotov, and A. V. Garbaruk, (2017). “Calculations of flow around airfoils using two-dimensional RANS: an analysis of the reduction in accuracy.” *St. Petersburg Polytechnical University Journal: Physics and Mathematics*, vol 3, pp. 15-21, March 2017. **[Online] Available:** <https://doi.org/10.1016/j.spjpm.2017.03.004> **Accessed:** March 2019.
- [35] M.O. Petinrin, and V. Onoja, “Computational Study of Aerodynamic Flow over NACA 4412 Airfoil.”, *British Journal of Applied Science & Technology*, vol. 21, no. 3, pp. 1-11, January 2017. **Accessed:** April 2019.
- [36] K. Yousefi, R. Saleh, and P. Zahedi, “Numerical Study of Flow Separation Control by Tangential and Perpendicular Blowing on the NACA 0012 Airfoil”, *International Journal of Engineering*, vol 7, pp. 10-24, February 2013. **Accessed:** April 2019.
- [37] D.C. Eleni, T.I. Athanasios, and M.P. Dionissios, “Evaluation of the turbulence models for the simulation of the flow over a National Advisory Committee for Aeronautics (NACA) 0012 Airfoil”, *Journal of Mechanical Engineering Research*. 2012; vol 4, issue 3, pp. 100-111, March 2012 **[Online] Available:** <https://doi.org/10.5897/JMER11.074> **Accessed:** April 2019.
- [38] Y. Jiao, and Y. Lu, “Parameter Optimization Research on Lift-enhancing of Multi-element Airfoil Using Air-blowing.”, *Procedia Engineering*. 99. Shanghai, September 24th-26th. 2014. **[Online] Available at:** <https://doi.org/10.1016/j.proeng.2014.12.510> **Accessed:** April 2019.
- [39] M. Yılmaz, H. Köten, E. Çetinkaya, Z. Coşar, “A comparative CFD analysis of NACA0012 and NACA4412 airfoils”, *Journal of Energy Systems*, vol 2, no. 4, pp. 145-159, December 2018. **[Online] Available at:** <https://doi.org/10.30521/jes.454193> **Access:** May 2019.
- [40] V. Kornilov, “Current state and prospects of researches on the control of turbulent boundary layer by air blowing”, *Progress in Aerospace Science*, vol 76, pp. 1-23, July 2015 **[Online] Available at:** <https://doi.org/10.1016/j.paerosci.2015.05.001> **Access:** May 2019.